UNIVERSITÀ DEGLI STUDI DI PALERMO

Dottorato di Ricerca in Medicina Sperimentale e Molecolare
Referente: Prof. Francesco Cappello
Dipartimento di Biomedicina Sperimentale e Neuroscienze Cliniche

Hsp60 levels and mitochondrial biogenesis in skeletal muscle after endurance training

Tesi di dottorato di:
Dott.ssa Claudia Sangiorgi

Tutor:
Chiar.mo Prof.ssa Valentina Di Felice

Co-Tutor:
Dott. Rosario Barone

TRIENNIO 2013-2015

I am grateful to all the people who supported me in this journey and patiently guided me through the new experiences. They helped me to face daily obstacles, giving me the opportunity to grow both in professional and personal field. Therefore, I wish to thank all teachers and colleagues of Department of Experimental Medicine and Clinical Neuroscience of University of Palermo. And a special thanks goes to Gerardo and my family.

List of contents

List of images

List of tables

1 INTRODUCTION

1.1 Skeletal muscle niche

Muscle tissue can differentiate in three forms: skeletal, cardiac or smooth muscle.

Skeletal muscle is part of musculoskeletal system, it is innervated by somatic motor nerves, then it is considered a voluntary muscle; it has a functionally unit that is responsible of the contraction. Smooth muscle that is found in the walls of hollow organs, and consists of small elongated cells that are not striated and are under involuntary control. Cardiac muscle that occurs only in the heart, it consists of small cells that are striated and under involuntary control.

The skeletal muscle is able to contract and cause movement but also to stop movement, such as resisting gravity to maintain posture. Muscle contraction requires energy produced by ATP broken down. This step produces heat, that is very noticeable during exercise.

Each skeletal muscle is an organ that consists of various integrated tissues: the skeletal muscle fibres, blood vessels, nerve fibres, and three layers of connective tissue that enclose it, and also compartmentalize the muscle fibres within the muscle. The epimysium wrap the entire muscle and separates it from other tissues and organs in the area, allowing the muscle to contract and to move independently. Inside each skeletal muscle its cellular units, the muscle fibres, are organized in fascicle, by a middle layer of connective tissue called the perimysium. Inside each fascicle, each muscle fibre is encased in a thin connective tissue layer of collagen called the endomysium.

The muscle fibres develop by fusion of individual myoblasts, they contain the cytoplasm, called sarcoplasm, that is surrounded by the sarcolemma. Into the sarcoplasm there are myofibrils, long narrow structures (1–2 μm in diameter) that represent the contractile machinery. Numerous nuclei are usually localized between the myofibrils and the sarcolemma. Myogenic satellite cells lie between the sarcolemma and the surrounding basal lamina.

The functional unit of a skeletal muscle fibre is the sarcomere, an highly organized structure consisting of myofilaments actin (thin filament), myosin (thick filament) and their regulatory proteins, troponin and tropomyosin, and other support proteins. Each sarcomere is bordered by structures called Z-discs to which the actin

myofilaments and its troponin-tropomyosin complex are anchored projecting toward the center of the sarcomere. The A-band consists of the thick filaments, together with thin filaments that interdigitate with, and thus overlap. The central region of the A-band is the H-zone, containing at the centre the M-line, where the thick filaments are linked together transversely. The I-band consists of the adjacent portions of two neighbouring sarcomeres, in which only thin filaments are present and anchored in the Z-disc. A third type of filament is composed of the elastic protein, titin.

When signal by a motor neuron arrive up to a skeletal muscle, Ca^{2+} entry into the sarcoplasm, bind to troponin so that tropomyosin can slide away from the binding sites on the actin strands. This allows the myosin heads to bind to these exposed binding sites and form cross-bridges, thin filaments and thick filaments slide on each other, then fibres contracts. This step requires ATP.

A number of proteins which are neither contractile nor regulatory are responsible for the structural integrity of the myofibrils: α-actinin, is a rod-shaped molecule which anchors the plus-ends of actin filaments from adjacent sarcomeres to the Z-disc; nebulin inserts into the Z-disc, associated with the thin filaments; desmin that is an intermediate filament protein characteristic of muscle and with plectrin forms a network that connects myofibrils together and the sarcolemma. Dystrophin is confined to the periphery of the muscle fibre, close to the cytoplasmic face of the sarcolemma, it binds to actin intracellularly and is also associated with a large oligomeric complex that links specifically with merosin, the α2 laminin isoform of the muscle basal lamina.

The fibres contain other organelles essential for cellular function, such as ribosomes, Golgi apparatus, mitochondria and a network of tubules and cisterns called triads. Tubular invaginations of the sarcolemma penetrate between the myofibrils, the lumen of these transverse (T-) tubules are thus in continuity with the extracellular space. The sarcoplasmic reticulum (SR) is a specialized form of smooth endoplasmic reticulum and forms a plexus of cisterns that expand into larger sacs, terminal cisterns, where they come into close contact with T-tubules, forming these structures called triads.

Skeletal muscles are composed entirely of fibres of the twitch type. The first type of fibres obtain their energy by aerobic oxidation of substrates, particularly of fats and fatty acids. They have large numbers of mitochondria; contain myoglobin, an oxygen-transport pigment related to haemoglobin. Such fibres have the function such as postural maintenance, in which moderate forces need to be sustained for prolonged periods. The other type of fibres have few mitochondria, little myoglobin, and store

energy as cytoplasmic glycogen granules. They produce energy through anaerobic glycolysis, a route that provides prompt access to energy but for a shorter period than oxidative metabolism. They are capable of brief bursts of intense activity.

Muscles that have a conspicuously red appearance are rich blood supply and high myoglobin content and they are characterized by a predominantly aerobic metabolism; whereas others have a much paler appearance, reflecting a more anaerobic character. These variations led to discern muscle into red and white types.

The red muscle are mainly consist by oxidative, slow twitch fibres, the white one by glycolytic, fast twitch fibres. Slow-contracting are defined type I fibres, that fast-contracting are defined type II fibres.

Molecular analyses have revealed that fibres may be further identified according to their content of myosin heavy-chain isoforms. Myosin heavy-chain I (MHCI) are generally oxidative fibres, myosin heavy-chain IIB (MHCIIB) largely rely on glycolytic metabolism, and myosin heavy-chain IIA (MHCIIA) are moderately oxidative and glycolytic,

Until the mid 20th century, the mechanisms responsible for the maintenance and repair of skeletal muscle were unclear. These issues were largely resolved with the discoveries that multinucleated muscle fibres were formed by the fusion of mononuclear precursors, myoblasts, and that in addition to the already differentiated muscle fibres, in the muscle, there are the undifferentiated cells, called progenitor cells.

The route of differentiation is favoured by myogenic determination factors Myf-5, myogenin, MyoD and Myf-6 (herculin) are a family of nuclear phosphoproteins. They have in common a 70-amino-acid, basic helix-loop-helix (bHLH) domain that is essential for protein–protein interactions and DNA binding. Outside the bHLH domain there are sequence differences between the factors that probably confer some functional specificity.

The myogenic factors do not all appear at the same stage of myogenesis (Buckingham et al 2003). In the somites, *Myf-5* is expressed early, before myotome formation, and is followed by expression of *myogenin*. *MyoD* is expressed relatively late together with the contractile protein genes. *Myf-6* is expressed transiently in the myotome and becomes the major transcript postnatally. Myogenin is crucial for the development of functional skeletal muscle, and that while neither Myf-5 nor MyoD is essential to myogenic differentiation on their own. *Myf-5* is expressed first but transiently, followed by *myogenin* and *MyoD*, and eventually *Myf-6*.

These molecular pathways are also essential in differentiation process of progenitor cells that promote growth and repair in adult muscle.

The most of these are Satellite cells located between the basal lamina and myofibre plasma membrane (Pannérec et al., 2012). They are mononucleated cells with myogenic potential, unlike differentiated fibres. This cell population presents specific markers such as Pax7 (transcription factor), N-CAM, M-cadherin, CD34 (membrane protein) (Biressi et al., 2010). Following muscle injury, satellite cells undergo asymmetric divisions leading to the formation of undifferentiated cells, which return to quiescence and thus replenish the satellite cell compartment, and differentiated myoblasts which form new myofibres (Pallafacchina et al, 2013).

Satellite cells grown *in vitro*, in differentiating medium, lose partly their self-renewal and regenerative capacity, when they are re-engrafted in a damaged muscle (Montarras et al., 2005). Thus, we might suggest that the surrounding environment is fundamental for satellite cells operation. Small vessels secrete IGF-1, fibroblast growth factor (FGF), hepatocyte growth factor (HGF), vascular endothelial growth factor (VEGF) that influence satellite cells located close to them (Sonnet et al., 2006). In turn, satellite cells differentiated in myoblasts promote angiogenesis in a positive feedback that allows a faster tissue repair: they attract fibroblasts for the following connective tissue expansion and they promote conversion of monocytes in anti-inflammatory macrophages that stimulate myogenesis and fibre growth (Arnold et., 2007). Vascular-mediated paracrine effects on the stem cells niche play a fundamental role on their response. Indeed, satellite cells ablation leads to a complete loss of muscle regeneration and to a defect in fibroblasts recruitment with consequent slowing in the regeneration of connective tissue (Murphy et al., 2011).

Several signalling pathways are involved in satellite cells proliferation, like cytokines, interleukin-4 and 6; while Wnt signalling, ligand of the membrane receptor Frizzled, decreases the proliferative capacity and promotes the differentiation of satellite cells to become fusion-competent myoblasts (Brack et al., 2007). On the other hand, Notch, a membrane receptor activated by the ligand Delta, seems to control the balance between satellite cells proliferation and differentiation (Brack et al., 2008).

In spite of this, there may be reports about non-satellite cell populations with myogenic capacity (Pannérec et al., 2012). For example, side population (SP) that have the capacity to reconstitute the hematopoietic lineage (Jackson et al.,1999; Asakura et al., 2002) and restore dystrophin expression and improve muscle function in mdx mice

(Gussoni et al., 1999). An additional population are Mesoangioblasts (Mabs), isolated from embryonic or postnatal muscle vasculature (De Angeli L. et al., 1999); finally, also Pericytes that contribute to postnatal muscle growth and repair (Dellavalle et al., 2011).

1.2 Muscle Wasting

Muscle wasting is defined as a weakening, shrinkage, and loss of muscle caused by disease or lack of use. It occurs usually in the context of many diseases and conditions which cause a decrease in muscle mass: inactivity or upon extended bed rest (which can occur during a prolonged illness) and cachexia. This derangement involves muscle proteins and it is characterized by an increase in protein catabolism and a decrease in protein synthesis.

Protein synthesis is regulated by two key factors: eukaryotic initiation factor 2 (eIF2) and factor 4F (eIF4F). The first is associated with a pathway GTP/GDP-dependent and it leads to an active translation, while there is a block of translation when eIF2 is phosphorylated. The latter drives to a correct starting of the translation; it results from the cooperation between eIF4E-4A-4G. In a cachectic subject phosphorylation of eIF2 (Eley, Russel, Tisdale, 2007) and eIF4E binding to 4E-BP1, the constitutive regulator of eIF4F complex (Eley, Tisdale, 2007), increase.

Protein catabolism may be due to the activation of the lysosomal system, cytosolic calcium-regulated calpains and mainly from the ATP ubiquitin-dependent proteolytic pathway. This degradation brings to loss of muscle fibres and later to atrophy. The lysosomal system is mainly responsible for the degradation of extracellular proteins and receptors. Pathway involving calpains attends in tissue injury and necrosis. The ubiquitin-proteasome pathway contributes to the degradation of myofibrillar proteins (Hasselgren et al., 2002).

The release of superoxide anions, hydrogen peroxides or nitric oxide can contribute to muscle wasting. These molecules can interact each other and generate more highly reactive products (Peroxynitrite and hydroxyl radical). This series of events can be set off by an inflammatory event and they culminate in oxidative stress. The increase of reactive oxidative species (ROS) promotes catabolism of muscle cells even more. A study conducted in C2C12 cells documented that ROS induces an up-regulation of E3-ubiquitin ligases (Li et al., 2003), accordingly grow up proteasome activity and degradation of myosin. In cancer cachexia MHC is an important target of

muscle wasting. It is reduced in protein form but steady in mRNA level, as it was established with an experiment of Lenk et al. where MHC immunoprecipitated with ubiquitin (Lenk et al., 2010).

The fast-twitch type II fibres (in *tibialis* anterior and *gastrocnemius*) are lost faster than slow-twitch type I fibres (in *soleus*) (Tisdale et al., 2009).

In skeletal muscle there are two muscle-specific E3 ligases: atrogin-1 (MAFbx) and Muscle RING-finger protein-1 (MuRF1) (Lokireddy et al., 2012). Both act on myofibrillar and intracellular proteins labelling them for degradation through the ubiquitin-proteosome system (UPS). Expression of atrogin-1 and MuRF1 are regulated by insulin growth factor-1 (IGF-1)/ phosphatidylinositol-3-kinase (PI3K)/ Akt pathway, Forkhead box protein O1 (FoxO1) and 3, nuclear factor kappa-light-chain-enhancer of activated B cells (NFkB) (Lokireddy et al., 2012).

Indeed muscle wasting is a direct consequence of circulating proteins produced by both the host and tumour.

Among these, a considerable factor is FoxO. In myotube, activation of FoxO3 stimulates both lysosomal and proteasome-dependent protein degradation (Tisdale et al., 2009). Glucocorticoids contribute to FoxO activation decreasing action of PI3K/Akt pathway that inactivates it by phosphorylation (Tisdale et al., 2009). It was highlighted in a study by Liu et al (Liu et al., 2007) on a cancer cachexia mice model, where the expression of Foxo-1 in normal and cachectic mice was reduced using silencing oligonucleotides: this caused an increase in skeletal muscle mass of the mice, an increase in the levels of myogenic differentiation factor (MyoD) and a decrease in the levels of Myostatin.

Myostatin, a Transforming growth factor beta (TGFβ) superfamily member, is the responsible factor for stopping growth of muscle tissue. It is further secreted by murine and human neoplasms. It seems that myostatin is involved in the generation of cancer cachexia. Murine C26 colon cancer cells release a vast amount of myostatin, and experiments conducted with C2C12 exposed to C26 conditional medium demonstrated that the tumour mass produces such an amount of myostatin that can trigger skeletal muscle wasting (Zhou et al., 2010). Probably because it blocks proliferation and differentiation of the cells, and induces a decrease in MyoD levels. Skeletal muscle in C26 tumour bearing mice also displayed elevated activity of the autophagy-lysosome pathway. In light of this, Lokireddy et al. (Lokireddy et al., 2012) asserted that "myostatin is a novel tumour factor".

The loss of muscle mass is also affiliated to an increased serum level of a tumour produced proteolysis-inducing factor (PIF). Indeed an administration of PIF in a normal mice bring to a rapid decrease in body weight and enhancement in mRNA of ubiquitin in the *gastrocnemius* and components 19S and 20S proteosome (Lorite et al., 2001). PIF activates a pathway that involves phospholipase A_2 (PLA_2) that produces arachidonic acid (AA) that in turn actives NADPH oxidase. This mechanism releases ROS and activates NFkB contributing to proteasomic degradation downstream (Tisdale et al., 2009).

Also cytokines are involved in muscle wasting. Costelli et al. (Costelli et al., 2002), using inhibitors for tumour necrosis factor- α (TNF-α) and interleukin 6 (IL-6) in rats bearing hepatoma, they prevented the depletion of muscle mass and reduced proteolysis (Fig.1) .

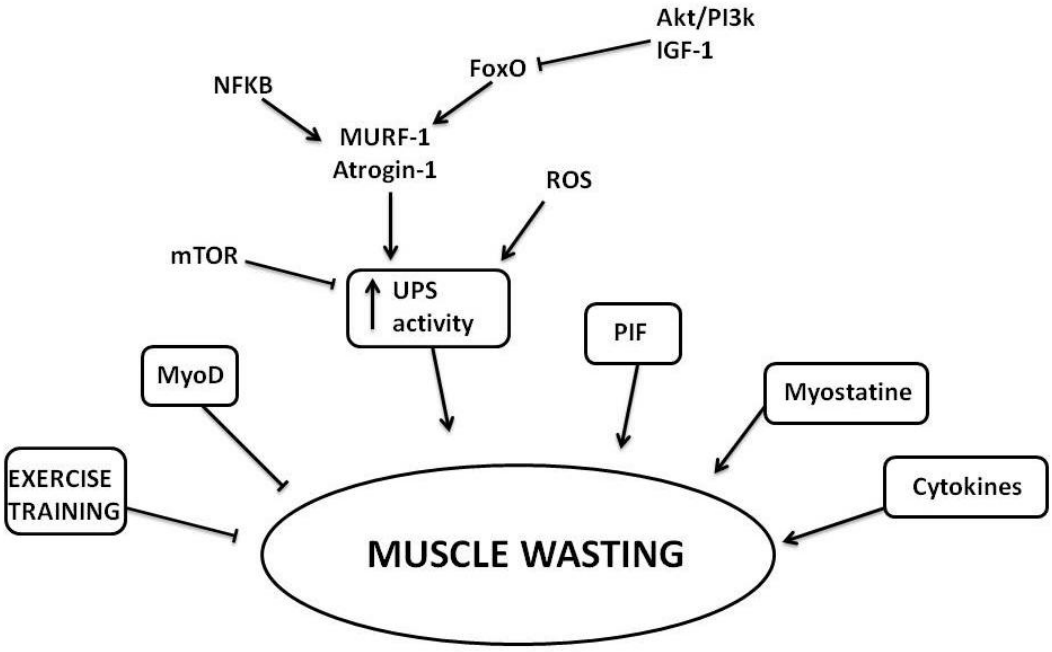

Fig. 1
Pattern of factors that originates the muscle wasting. (Sangiorgi C et al.: Muscle wasting and cardiac muscle damage in cachectic patients. Euromediterranean Biomedical Journal, 2013)

Opposite to these negative factors, IGF-1 can positively regulate muscle mass stimulating protein synthesis.

1.2.1 Sarcopenia and Cachexia

Sarcopenia and Cachexia are both conditions characterized by loss of skeletal muscle. The first is associate with aging without any declared disease, the second one, instead, is linked to chronic diseases, cancer, inflammatory conditions, heart failure. They are not always totally independent. In some cases, sarcopenia e cachexia can coexist or interact. Also, physical inactivity is exacerbated by both chronic disease and age, then it contributes to muscle wasting in some patients. Physical activity, therefore, could contribute to maintenance of skeletal muscle mass (Bowen et al., 2015).

In sarcopenia insulin sensitivity is impaired, then, the release of IGF-1 and expression of Akt and mammalian target of rapamycin (mTOR) is reduced. As a consequence protein synthesis and proliferation of satellite cells are less stimulated, and also, Peroxisome proliferator-activated receptor-γ (PPAR-γ) co-activator 1α (PGC1α) signaling is reduced (Wenz et al., 2009). On the other side, there's also an increase in protein degradation due to calpain system rather than to UPS (Dargelos et al., 2007). While autophagy declines with age (McMullen et al., 2009), muscle markers of apoptosis are significantly increased in old compared to young individuals, as it is suggested by Wenz T. et al. in a work of 2014, where the overexpression of PGC1α in aged mice reduces mitochondrial impairments, apoptosis and also muscle wasting (Wenz et al., 2009). Also satellite cells numbers and regenerative capacity are reduced in relation to aging; likely, this is determined by the expected increase of myostatin with age, that has been demonstrated to impair satellite cells regeneration (McCroskery et al., 2003). Overall this move towards an alteration of the subtle balance pro-oxidant and anti-oxidant enzymes in favor of the first, determining an increase of ROS and damage of mitochondrial DNA (Tanhauser et al., 1995). It seems that the main impairment is about superoxide dismutase (SOD) expression and activity (Sakellariou et al., 2014).

Regarding cachexia, the definition that scientists and clinicians agreed in the cachexia consensus conference in 2006 in Washington (DC) describes cachexia as a "complex metabolic syndrome associated with underlying illness and characterized by loss of muscle with or without loss off fat mass" (Evans et al., 2008). In cachectic condition the main cause that brings to muscle wasting is the increase in UPS activity. Mice with cancer cachexia colon-26 tumour-induced show a reduction mainly in myosin heavy chain causing a skeletal and respiratory muscle wasting, increasing also risk of respiratory failure (Roberts et al., 2013). This is linked to the growing in MURF-

1 and MAFbx activity, on the one side, to the down-regulation of de-ubiquitinases (Wing et al., 2013). The consequence of these events is, as previously said, the intensification of ROS release and, consequently, of pro-inflammatory factors as TNF-α, IL-6 and cytokines in general. In addition, however, in 70% of cachectic subjects, there's also low testosterone level and consequently, decrease in IGF-1 mRNA, in myofibrillar protein synthesis and kinases phosphorylation (White et al 2013). Regarding myostatin, it is overexpressed and acts suppressing Akt, reducing protein synthesis, promoting FoxO transcription, then, encouraging protein degradation. Some evidences propose follistatin like inhibitor of myostatin, therefore, muscle wasting in cachexia (Cohen et al.2015).

1.2.2 Training like treatment

The attempt to improve the conditions of a cachectic subject with real medical treatments don't give great results to reduce cachexia effects on lean mass reduction. Appetite stimulants, such megestrol acetate, were used, but gain in weight was due to an accumulation of fat rather than body mass (Tisdale et al., 2009). Another attempt was cyproheptadine, a histamine antagonist, that improved in appetite but did not avoid weight loss. Corticosteroids also enhance appetite, performance and sensation of well-being but they did not have positive effects on body weight (Tisdale et al., 2006). We know that, also, growth hormone (GH) influences in a positive manner muscle mass but its clinical efficacy has not been demonstrated yet (Osterziel et al., 1998).

Moreover cachexia can be treated with an inhibitor of gene transcription of TNF (Pentoxifylline), with anti-cytokine antibodies and cytokine receptor antagonists. Anti-inflammatory/anabolic cytokine, like interleukin-15 (IL-15), has a key role in a decrease in protein degradation and DNA fragmentation (Muliawati et al., 2012) .

Until now, in recovery of loss mass, the treatment that brings the most positive results is exercise training. Also, recently it has been suggested to slow the progression of several cancer forms and to increase cancer survivorship by decreasing the risk of recurrence (Courneya and Friedenreich, 2007).

Exercise training is able to decrease myostatine and cytokines expression in skeletal muscle. It may reduce pro-inflammatory cytokine expression, mainly of TNF and IL-6 (Smart et al., 2011) and the expression of myostatin in skeletal muscle (Lenk et al., 2012). The anabolic component of exercise training increases activation of

antioxidant enzymes. Resistance training, moreover, induces significant phosphorylation on mTOR favoring protein synthesis (Lenk et al., 2012).

A regular physical activity can improve quality of life and it has positive effects on the chance of survival. Probably the efficacy of exercise training is linked to the adult stem cells (ASC) of skeletal and cardiac muscle tissue, but also to the molecular pathways that arising by training.

Physical activity, with its relative contracting skeletal muscle, generates an increase in the rate of reduction of oxygen. This brought to an increase of reactive oxygen species (ROS) and reactive nitrogen species (RNS) production, as demonstrated by Davies et al. in 1982 and Balon &Nadler in 1994, respectively (Davies et al., 1982; Balon et al., 1994).

On the other hand it gives also the production of antioxidant enzymes, as MnSOD (superoxide dismutase manganese dependent) (McArdle , Van Der Meulen et al., 2004) or transcription factor as PGC1α that contribute to slow down muscle wasting by sarcopenia restoring protein synthesis and limiting protein degradation acting on myostatine and FoxO expression. The resistance exercise training (RET) improves muscle mass and strength by increasing fibres cross-section area and number of myofibrils (Atherton et al., 2012). In particular, it stimulates PGC1-α4 isoform that prevent cancer cachexia, in mice, by activating IGF-1 and repressing myostatin.

Further, training pushes cyto-protective proteins production, like for example proteins of heat shock proteins (HSPs) family (McArdle et al., 2004).

1.3 Mitochondrial biogenesis

Mitochondria from fast type II fibres have properties that promote higher levels of ROS production, rather than slow type I fibres (Anderson et al., 2006). Furthermore, you know that increase in ROS and RNS production is involved in signalling pathways that brought to muscle adaptation in response to endurance exercise training.

An important adaptation that follows the training of skeletal muscle is the increase in mitochondrial muscle fibre due to mitochondrial biogenesis. This event originates since gene products transcription, from both the nuclear and mitochondrial genomes.

PGC1α has been shown to be protagonist and fundamental regulator in mitochondrial biogenesis. It interacts with several transcription factors and nuclear

receptors involved in both nuclear- and mitochondrial-encoded genes transcription required in organelle synthesis (Powers et al., 2011).

PGC1α transcription is positively controlled by high cellular levels of ROS, through AMP-activated protein kinase (AMPK) pathways (Irrcher et al., 2009). Nuclear factor-kB (NF-kB), adjusted in turn by ROS levels, would influence the expression of PGC1α, thanks to binding site contents in its promoter (Irrcher et al., 2008). Moreover, p38 mitogen-activated protein kinases (p38 MAPK) and AMPK are capable of phosphorylating PGC1α at a variety of amino acid residues, which results in a more stable and active PGC1α protein (Fig.2) (Powers et al., 2011).

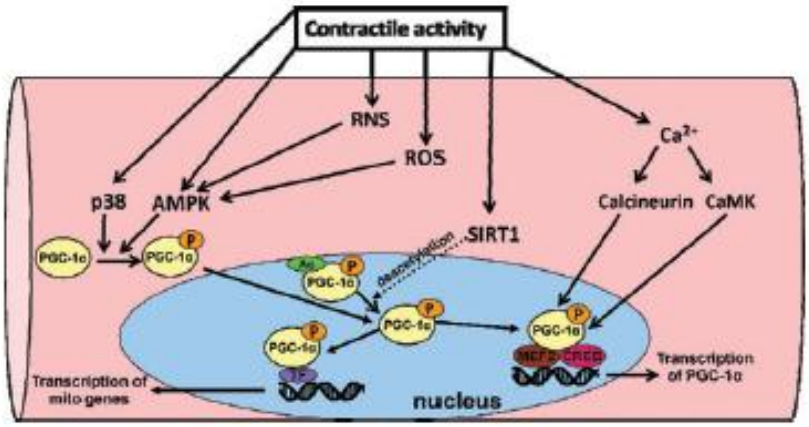

Fig. 2
Steps leading to NF-κB activation and signalling in cells. (Scott K. Powers et al. 2011. Reactive oxygen and nitrogen species as intracellular signals in skeletal muscle J Physiol 589.9)

Then, PGC1α is induced by exercise and it causes, in addition to biogenesis, also fibre type switching, stimulation of fatty acid oxidation, angiogenesis and resistance to muscle atrophy (Arany et al., 2008).

In mouse and human skeletal muscle and adipose tissue, the *PGC1α* gene can be driven by two different promoters. The proximal promoter, located in canonical exon 1 (exon 1a) and the distal one sited in the alternative exon 1 (exon 1b) located at 13.7 kb upstream from the exon 1a of the *PGC1α* gene (Fig.3) (Miura et al., 2008).

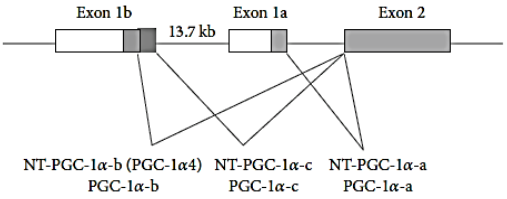

Fig. 3
Schematic structure of the 5'-region of the murine *PGC1α* gene. (Xingyuan W. et al. 2014. Effect of Exercise Intensity on Isoform-Specific Expressions of NT-PGC1α mRNA in Mouse Skeletal Muscle. Hindawi Publishing Corporation).

Exon 1b presents two different splice sites. PGC1 α-b and PGC1 α-c isoforms derive by alternative splicing of these two different sites to the exon 2.

Previous studies have shown that alternative splicing between exons 6 and 7 of the *PGC1α* gene produces an additional transcript encoding the N-terminal isoform of PGC1α (NT-PGC1α), which consists of 267 amino acids of PGC1α and 3 amino acids from the splicing insert (Fig.4).

Fig. 4
The schematic diagram of amino acid sequences of NT-PGC-1α-a, NT-PGC-1α-b, and NT-PGC-1α-c and PGC-1α-a, PGC-1α-b, and PGC-1α-c. (Xingyuan W. et al. 2014. Effect of Exercise Intensity on Isoform-Specific Expressions of NT-PGC-1α mRNA in Mouse Skeletal Muscle. Hindawi Publishing Corporation)

The three NT-PGC1α mRNA isoforms (NT-PGC1 α-a, NT-PGC1 α-b, and NT-PGC1 α-c) are coexpressed with three PGC1α isoforms and regulate thermogenic and mitochondrial gene expression in response to cold stress (Wen et al., 2014).

1.4 HSPs in stress response

Also chaperon proteins are among molecules involved in pathways induced by high levels of ROS. They are traditionally known like molecules that facilitate synthesis, folding and assembly of proteins (Moseley et al., 1997). Nevertheless, it's

also demonstrated that they have protective effects against stress: indeed they are found in response to heat-shock stimuli and other kind of cellular stress (Locke et al., 1995). The main function of skeletal muscle is to permit the movement of the body, during this function, it is subjected to several tissue changes, including the induction of HSPs, which are also upregulated, in skeletal muscle, after stress (Fehrenbach et al., 1999).

Increase in the levels of HSPs is regulated by a specific DNA sequence, named heat shock element (HSE), located upstream the coding regions of various HSP genes (Morimoto et al., 1992), that is a binding site in the promotor region for a specific protein known as heat shock transcription factor (HSF). In mammals we have HSF1, activated by several stressors like heat, oxidative stress and denatured proteins; HSF2 that seems to regulate protein expression and cell differentiation. HSF1 and HSF2 isoforms can be transcribed by alternative splicing in a tissue-dependent manner (Goodson et al., 1995). In unstressed cells, HSF1 is present in a monomeric form that is enable to DNA binding activity. After exposure to stresses, HSF1 acquires a trimeric state and the DNA-binding activity, then it accumulates in the nucleus and binds to the HSE (Sorgen et al., 1991).

It has been suggested that HSP themselves may negatively regulate HSP gene expression (Fig. 5) (Locke, 1997). When the HSP gene is activated, increases the pool of unbound HSP and the possibility of complex formation with activated HSF: the binding of HSP to HSF will inhibit further DNA-binding of HSF and consequently, will decrease HSP transcription.

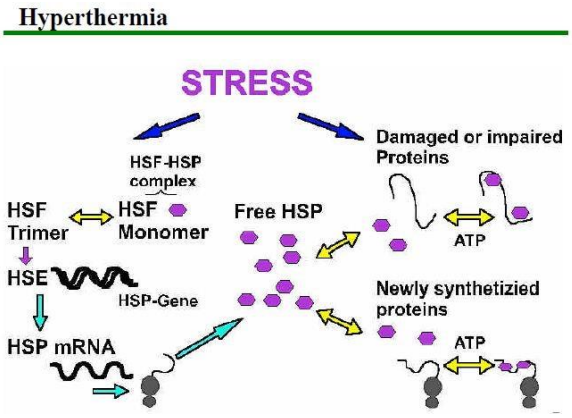

Fig. 5
Stress-dependent regulation of HSP-gene expression by HSF (left), and functions of HSP as chaperone of denaturated proteins or of nascent proteins (right), and the feed-back regulation of HSP-HSF-complex (Yuefei Liu et al. 2001. Changes in skeletal muscle heat shock proteins: pathological significante. Frontiers in Bioscience 6, d12-25

HSP expression is not only organ or tissue specific (Flanagan et al., 1995; Manzerra et al., 1997), but also muscle fibre type specific (Neufer et al., 1996).

Oishi Y. et al subjected the *soleus* and *plantaris* muscle of rats to a single bout of elevated temperature for 1h. They observed different response of some of HSPs family, in slow fibre of *soleus* and fast ones of *plantaris* (Oishi et al., 2003).

Fibres with type I, IIa or IIb myosine heavy chain have respectively decreasing mitochondrial content. Mitochondria are the location of several HSP proteins like Hsp60; Hsp10 that assists the latter in its function; mitochondrial Hsp70, also known like 75kDA glucose-regulated protein (GRP75) (Welch et al., 1992). Indeed, Hsp70 protein is mainly present in type I fibres, almost nothing in type II.

A chronically stimulation (10Hz), in a muscle like tibialis anterior (TA), make reduce amounts of type IIb MHC gaining type IIa fibres. These changes could represent the input for molecular pathways that enhance expression of stress proteins (Ornatsky et al., 1995).

1.5 Hsp60

Among stress proteins, Hsp60 generates great interest. It is mainly known for its function like chaperons, but its levels are found overexpressed in stress conditions like tumours (Campanella et al., 2012) or chronic diseases. In addition to its usual mitochondrial localization, it was found also in cytosolic and extracellular environment (Cappello et al., 2008). This differentially localization could be possible its interaction with several physiological elements.

Then, Hsp60 could be involved in many of molecular pathways originated by exercise training and the resulting oxidative stress; indeed, there are already proven correlations between hsp60 and physical training, in literature.

Mattson and its collaborators observed the trend of HSPs in skeletal muscle after endurance training. With their results, for the first time in literature, they showed a chronically increase in Hsp70 and Hsp60 in *plantaris* (IIa/IIx fibres type) rat muscle but not in *soleus* (I fibres type) (Mattson et al., 2000). It is also found that increase of Hsp60 coincides with the rise in citrate synthase activity in the *plantaris*. This suggests a collaboration of the two proteins to support typical muscle adaptations to endurance activity, in which, mitochondrial activity is clearly involved. Other evidences about the relation between Hsp60 and exercise training reproduce the increase of the protein in

soleus of rats (Fisher 344) after endurance training, as well as in right and left ventricle of heart (Samelman et al., 2000).

In human, the analysis of the *vastus lateralis* muscle (I/IIa/IIb fibres type) biopsies shows an increase in Hsp60, αβcrystallin and MnSOD in trained rather than in untrained subjects (Morton et al., 2008). In particular, the authors explain the up-regulation of Hsp60 with the need to protect mitochondrial proteins against damage and to facilitate protein import and folding in mitochondrial biogenesis exercise-induced. More recently, in 2013, another research group worked with human *vastus lateralis* and they found an uniform expression of Hsp60 in I/IIa/IIx fibres type, in the various untrained, resistance and endurance trained subjects (Folkesson et al., 2013).

1.6 AIMS

The aims of this study were to evaluate the effects of endurance exercise on Hsp60 and PGC1α expression levels and their interaction on different skeletal muscle fibres in a mice model, and the molecular pathway triggered by Hsp60 overexpression in an *in vitro* model of myoblasts.

We hypothesized that an increase in Hsp60 should not be the same in all fibre types considering their variety, and should be accompanied by changes in PGC1α and increased mitochondrial numbers. We planned experiments to dissect the molecular interactions involving Hsp60 in muscle. Also, we focused on other molecules involved in the pathways lead by p38 and AMPK, which represent key steps in PGC1α expression and activation in skeletal muscle fibres as stress response.

To test our assumption, we first performed a comprehensive assessment of Hsp60 levels in sedentary and trained mice, comparing different type of fibres. Moreover, using a short-term overexpression of Hsp60 in cultured myoblasts, we studied a correlation between Hsp60 overexpression and PGC1 α1 activation.

2 MATERIALS AND METHODS

2.1 Animal model

BALB/c AnNHsd mice, obtained from Harlan Laboratories, Srl (Udine, Italy) were housed under a 12:12-hour light-dark cycle, provided with free access to food and water; they were free to move inside the cages. All animal experiments were approved by the Committee on the Ethics of Animal Experiments of the University of Palermo and adhere to the recommendations in the Guide for the Care and Use of Laboratory Animals by the National Institute of Health (NIH). All experiments were performed in the Human Physiology Laboratory of the Department of Experimental Biomedicine and Clinical Neurosciences of the University of Palermo, which was formally authorised by the Italian Ministry of Health (Roma, Italy).

Seventy-two young (7-weeks old) healthy male mice, were divided in two experimental groups: sedentary (SED) or trained (TR). The TR mice were trained according to a progressive endurance training protocol (TR_P) for rodents as previously performed in our lab (Di Felice et al., 2007) while SED mice did not perform any supervised running activity. Every two weeks, all mice were weighed, and their strength was measured. Forty-eight hours after the last training session, eight mice for each group were sacrificed via cervical dislocation after 15, 30 and 45 days. The group of posterior muscles (*gastrocnemius*, *soleus* and *plantaris*) of the hindlimbs were dissected and preserved in liquid nitrogen (right hindlimb) or embedded in paraffin (left hindlimb) to evaluate the morphological and molecular changes.

For the cachexia related experiments, seven mice were inoculated with a frozen fragment of solid C26 tumour derived from colon tumour mass of mouse. Tumour mass was token from these animals to inoculate the experimental mice with fresh fragments.

Six weeks before the inoculation, adult (A) male (M) and female (F) mice were randomly assigned to one of the experimental conditions as follow: sedentary (SED), progressive training (TR_P), low intensity training (TR_L), moderate intensity training (TR_M) and high intensity training (TR_H). All trained mice performed the TR_P as first training protocol to create a progressive adaptation to the exercise and they were underwent to one of the other training program (TR_L, TR_M or TR_H) after tumour inoculum.

The groups were identified with the following acronyms: AM-SED/SED; AM-SED/TR_p; AM-TR_p/TR_l; AM-TR_p/TR_m; AM-TR_p/TR_h; AF-SED/SED; AF-SED/TR_p; AF-TR_p/TR_l; AF-TR_p/TR_m; AF-TR_p/TR_h.

A first set of experiments for cachexia involved 20 mice (3-months old) for each group (n=200). They were maintained until the natural death, to evaluate the survival. Body mass, tumour size and survival were monitored five days per week after inoculation. Tumour growth was calculated as the number of days passed from the inoculation to the palpable tumour under the skin. Cachexia, like loss of 15-20% of body weight and survive in a state of cachexia, was also evaluated as the number of days passed from the rise up of cachexia to the death.

2.2 Endurance training

A motorized Rota-Rod (Rota-Rod; Ugo Basile, Biological Research Apparatus, Comerio Varese, Italy) was used to train the mice accord to TR_P, TR_L, TR_M, TR_H endurance protocols (Table1).

Endurance training protocols.								
	TR_P		**TR_L**		**TR_M**		**TR_H**	
Week	**Time (min)**	**Speed (m/min)**	**Time (min)**	**Speed (m/min)**	**Time (min)**	**Speed (m/min)**	**Time (min)**	**Speed (m/min)**
1	**15**	**3.2**	**30**	**3.2**	**60**	**4**	**75**	**4**
2	**30**	**3.2**	**30**	**3.2**	**60**	**4**	**90**	**4**
3	**30**	**4**	**30**	**3.2**	**60**	**4**	**90**	**4.8**
4	**45**	**4**	**30**	**3.2**	**60**	**4**	**105**	**4.8**
5	**60**	**4**	**30**	**3.2**	**60**	**4**	**120**	**4.8**
6	**60**	**4.8**	**30**	**3.2**	**60**	**4**	**120**	**4.8**

Table 1
Endurance training protocols for mice. Progressive training (TR_P), low intensity training (TR_L), moderate intensity training (TR_M) and high intensity training (TR_H).

2.3 C26 tumour

C26 tumour mass derived from colon tumours induced and transplanted in different inbred mouse strains. It was originally defined as an undifferentiated Grade IV carcinoma (Corbett et al., 1975). In previous experiments, a sample of its cells was inoculated in BALB/C mice and it resulted highly tumourigenic and with little capacity to metastasize and an high percentage of C26-inoculated mice went against to death (Sato et al., 1981). The histological analysis showed C26 as a partially encapsulated, anaplastic carcinoma with cells different in size and a considerable vascularization sufficient to advance tumour growth (Aulino et al., 2010) .

C26 tumour promotes protein catabolism increasing atrogin-1 e MuRF1 activity (Acharyya et al., 2005). So it cause loss of adipose and skeletal muscle tissue, for this reason it's considered an appropriate model to investigate cachexia mechanisms (Tanaka et al., 1990) .

In our experiments, a solid fragment of about 2 mm^3 was subcutaneously implanted in BALB/C mice, upon the haunch. Around 10^{th} days it was visible as protrusion under skin that caused ulcers occasionally. From our histological observation it's no more visible capsules-like structures and it expresses more vimentin than keratin that is the typical epithelial marker.

2.4 Cell Culture Methods

C2C12 mouse adherent myoblasts were grown in High glucose Dulbecco's modified Eagle's medium (DMEM) supplemented with 20% fetal bovine serum (FBS), sodium pyruvate, L-glutamine, penicillin, and streptomycin (proliferation medium) at 37 °C in a humidified atmosphere with 5% CO2.

2.4.1 Bacterial Transformation

XL10-Gold ultracompetent cells (Agilent technologies 200315) are deficient in all known restriction systems [D(mcrA)183 D(mcrCB-hsdSMR-mrr)173] and in endonuclease (endA).

Bacterial cells are placed on ice and an aliquot 100 µl of cells is gently mix, into a pre-chilled tube, with 4 µl of the β-ME mix provided with these bacterial batches.

The cells incubate on ice for 10 minutes are swirling gently every 2 minutes, after, 50 ng of the experimental DNA are added to the aliquot. This mixture is incubated on

ice for 30 minutes after which we give it a Heat-pulse in a 42°C water bath for 30 seconds followed by an incubation on ice for 2 minutes. We add 0.9 ml of preheated (42°C) LB-broth and incubate the tubes at 37°C for 1 hour with shaking at 225-250 rpm.

Three-hundred microliters of this transformation mixture are plated on LB agar plates containing the appropriate antibiotic (Kanamycin for pCMV6-Entry-HSPD1, Ampicillin for pcDNA 3.1-mok), incubated at 37°C overnight.

2.4.2 Plasmid extraction

The grown colonies are inoculated each in 500 ml of LB-broth and incubated overnight. From this bacterial culture, plasmid DNA is isolated using the QIAGEN Plasmid Maxi Kit®, which is based on a modified alkaline lysis procedure. Plasmid DNA is bound by an anion-exchange resin contained in columns provides with kit. The DNA pellet was washed two times with 70% ethanol and dissolved in 30 µl 1x TE buffer, according to the manufacturer's protocol.

2.4.3 Transfection

Plasmids were transfected using Lipofectamine® 2000 Reagent according to the manufacturer's instructions.

Briefly, C2C12 cells were plated 1 day before transfection in 6-well dishes ($5x10^4$ cell/well).

On the day of the transfection, the cells were 70% confluent.

3.5 µg plasmid DNA (pCMV6-Entry-HSPD1 for overexpression of Hsp60 and pcDNA 3.1-mok like negative control) was diluted in 150µl of Opti-MEM Medium (without FCS, sodium pyruvate, L-glutamine, penicillin, and streptomycin) and mixed with 6 µl of Lipofectamine diluited in 150 µl of Opti-MEM. The mixture was added to cells grown. After 7–8 h, Opti-MEM and FBS was added to a final concentration of 20% in a final volume of 2ml.

Hsp60 siRNA (m) (sc-35604, Santa Cruz) was administered according to siRNA Reagent System (sc-45064, Santa Cruz) protocol using a mixture of 8µl siRNA duplex diluited in 100µl Tranfection Medium, with 8µl siRNA Tranfection Reagent diluited in 100µl Tranfection Medium. The siRNA neg-control is used in the same way. After 7 hours was added 1 ml of normal growth medium. The cells were incubated for 48 h.

To extract proteins and RNA, cells from each well were re-plated into a new 6-well dish and incubated for another 24 h in proliferation medium.

For immunofluorescence analysis, 10^4 cells/well were plated in chamber slides and after 24h cells were fixed with 4% glutaraldehyde and icy methanol.

2.4.4 Treatment with conditioned medium

The day after transfection, cells received fresh medium. The medium was taken 24h after and it was put in 6-wells plates with 70000 cells (C2C12) for well, to see the effect of factors released in the medium by transfected cells. RNA, to perform Real Time PCR, was exacted from the 3 kind of treatment (C2C12-medium, pcMV6-Hsd1-medium, pcDNA-medium) at different times: 0h, 6h, 24h, 48h.

2.5 Total RNA and DNA isolation

The total RNA and total DNA (genomic and mtDNA) were extracted using Trireagent (Sigma®) according to the manufacturer's instructions, by cryopreserved samples of transfected cells and muscles of trained and sedentary mice.

Tissue samples were then homogenized in TRI REAGENT (1ml for 50-100 mg of tissue) and subsequently centrifuged at 12000 x g for 10 minutes at 4°C to remove the insoluble material. 0,2 ml of chloroform was then added to the samples. After 15 minutes, the mixtures were centrifuged at 12000 x g for 15 minutes at 4°C, to separate the RNA (aqueous phase) from proteins (red organic phase) and DNA (interphase).

The aqueous phase was transferred to a fresh tube to which 0,5 ml of isopropanol was added. After 10 minutes, the samples were centrifuged at 12000 x g at 4°C. The supernatant was removed and the RNA pellet was added to 1 ml of 75% ethanol and then shaken. The mixture was centrifuged at 7500 x g for 5 minutes at 4°C. The RNA was eluted from the filter in 50µl of RNase-free H2O. The RNA extract obtained was stored at -20 ° C until use.

In the restant part was added 100% ethanol and the resulting pellet was washed with 0.1 Trisodium Citrate, suspended in 75% ethanol, dried under vacuum and dissolved in 8mM NaOH. 0.1 M HEPES was used to get a pH 8.4, more suitable for PCR analysis.

Concentration of samples were calculated with spectrophotometric analysis using NanoDrop 2000 UV-Vis Spectrophotometer.

2.6 Reverse Transcription PCR

Reverse transcription was performed using the ImProm-II Reverse Transcriptase Kit (Promega, Madison, WI, USA) according to the manufacturer's instructions.

The *oligo*, previously placed at 60° C for 5', was complexed with 300 ng of RNA extracted, in a final volume of 5µl in a first step (Table 2) in the thermocycler.

70°C	**10'**
4°C	**5'**

Table 2
First step reverse transcription PCR parameters.

To this volume were added 15µl of Mix (containing 5x Reaction buffer, MgCl2, dNTPs, RNase Inhibitor, Reverse transcriptase and H2O DNAse / Range free), then each sample has undergone a second step (Table 3) in the thermocycler. In this step, the RNA is copied in cDNA.

25°C	**5'**	**annealing**
50°C	**60'**	**extension**
70°C	**15'**	**Inactivation Reverse Transcriptase**
4°	∞	

Table 3
Second step reverse transcription PCR parameters.

2.7 Quantitative real-time PCR (qRT-PCR)

The cDNA was amplified using the primers in Table 5 with GoTaq® qPCR Master Mix kit (A6001, Promega Corporation, USA) and the protocol for thermal cycler (Rotor-Gene™ 6000, QIAGEN) described in Table 4.

95°C	2’	Hot-Start Activation	1 cycles
95°C	15’’	Denaturation	45 cycles
T° annealing primers	60’’	Annealing/ Extension	
60–95°C		Dissociation	1 cycles

Table 4
Quantitative real-time PCR (qRT-PCR) parameters.

The level of trascripted, of our primers (Table 5), was normalized to Glyceraldehyde 3-phosphate dehydrogenase (GADPH) degree. Changes in transcript level were calculated using the $2^{-\Delta\Delta Ct}$ method.

Primer	Target Sequence	Forward	Reverse
PGC1 tot	PubMed PMID: 23217713 (ref)	5’-TGATGTGAATGAC TTGGATACAGACA-3’	5’-GCTCATTGTTGTA CTGGTTGGATATG-3’
PGC1 a1	PubMed PMID: 23217713 (ref)	5’-GGACATGTGCA GCCAAGACTCT-3’	5’-CACTTCAATCCA CCCAGAAAGCT-3’
PGC1 a2	PubMed PMID: 23217713	5’-CCACCAGAATG AGTGACATGGA-3’	5’-GTTCAGCAAG ATCTGGGCAAA-3’
PGC1 a3	PubMed PMID: 23217713	5’-AAGTGAGTAAC CGGAGGCATTC-3’	5’-TTCAGGAAGAT CTGGGCAAAGA-3’
PGC1 a4	PubMed PMID: 23217713	5’-TCACACCAAA CCCACAGAAA-3’	5’-CAGTGTGTGT ATGAGGGTTGG-3’
HSP60_Mus	MGI:MGI:96242	5’-ACGATCTATT GCCAAGGAGG-3’	5’-TCAGGGGTTG TCACAGGTTT-3’
GADPH_Mus	MGI:MGI:95640	5'-CAAGGACACT GAGCAAGAGA-3'	5'-GCCCCTCCTG TTATTATGGG-3'

Table 5
Primers for quantitative real-time PCR (qRT-PCR) list.

2.8 mtDNA Copy Number Analysis

This method compares the levels of nuclear to mitochondrial DNA (mtDNA), in a DNA sample mtDNA. Copy number was quantitatively analyzed using GoTaq QPC kit (A6001, Promega Corporation, USA) real-time PCR (Applied Biosystems).

The genes mt-cyt_b and mt-12s as the mitochondrial marker ones, Becn-1 gene was used as the nuclear marker to standardize mtDNA copy number to diploid chromosomal DNA content.

Resultant Cts obtained from the Real-Time instrument are used to represent the level of each gene. Both the mitochondrial genes mt-12S and mt-Cyt_b are compared to the nuclear one, Becn-1 (Table 6).

Primer	Target Sequence	Forward	Reverse
BECN1_m	template MGI databse ID OTTMUSG00000002791	5'-CGAGTGCCTT CATCCAAAAC-3'	5'-GTCCTGGCAC CTCTCTAATG-3'
mt-Cytb_m	template MGI database ID 17711	5'-TAGCAATCGT TCACCTCCTC-3'	5'-TGTAGTTGTC TGGGTCTCCT-3'
mt_12s_m	template MGI database ID MGI:102493	5'-GATAAACCCC GCTCTACCTC-3'	5'-CATTGGCTAC ACCTTGACCT-3'

Table 6
Primers for quantitative real-time PCR (qRT-PCR) list.

Copy numbers were calculated based on the ΔCt of the matched mitochondrial to nuclear DNA Cts. To calculate copy number, the average of Set 1 = (mt-12S/BECN1) and Set 2 = (mt-Cyt_b/BECN1) ratios were determined. The individual ratios from Set 1 and Set 2 were used to calculate N = 2ΔCt where ΔCt1 = CtNucl - CtMito1 and ΔCt2 = CtNucl - CtMito2.

2.9 Immunoblotting

Samples, mice muscles and cells, were homogenized by lysis buffer (200 mM HEPES, 5 M NaCl, 10% Triton X-100, 0.5 M EDTA, 1 M DTT, 0.25 g Na-deoxycholate, 0.05 g SDS) supplemented with Protease Inhibitor Cocktail (Sigma-Aldrich, USA) in an ice-bath temperature, using also a hand plastic pestle for muscle.

The homogenates were centrifuged at 13000xg for 15 minutes at 4°C and the supernatant fractions (total lysate) were stored in -80°C freezer. The protein concentrations were quantified spectrophotometrically according to Bradford using bovine serum albumin (BSA, Sigma-Aldrich, USA) as the standard.

The proteins were separated by 12% SDS-PAGE and electrophoretically transferred to a nitrocellulose membrane 0.45 μm (Bio-Rad Laboratories, Inc. Germany). The membrane was incubated in a blocking solution containing 5% bovine serum albumin (BSA, Sigma-Aldrich, USA) in Tris-buffered saline (20 mM Tris, 137 mM NaCl, pH 7.6) containing 0.05% Tween-20 (T-TBS) for 1 h at RT.

Next, the membrane was further incubated in a primary antibody, anti-Hsp60 (diluted 1:1000, mouse monoclonal antibody ab13532, Abcam, UK), anti-glyceraldehyde-3-phosphate dehydrogenase (GAPDH - diluted 1:3000, rabbit polyclonal antibody ADI905784, Enzo Life Sciences, USA), anti-PGC1α (diluted, 1:1000, mouse monoclonal antibody ST1202, Calbiochem, USA), anti-Hsp70 (diluted, 1:1000, mouse monoclonal antibody C92F3A-5, Santa Cruz Biotechnologies, USA), or anti-Alix (diluited, 1:500, mouse monoclonal antibody sc-53538 Santa Cruz Biotechnologies, USA), in T-TBS containing 0.5% BSA overnight at 4°C. The following day, the membrane was washed with T-TBS and incubated with an HRP-conjugated secondary antibody (anti-rabbit NA934V, or anti-mouse NA931, Amersham Biosciences, USA) diluted in T-TBS containing 0.5% BSA for 1 h.

The detection of the immunopositive bands was performed using ECL Western Blotting Detection Reagent (Amersham Biosciences) according to the manufacturer's instructions.

The detected bands were analysed using ImageJ software version 1.41 (NIH, USA; http://rsb.info.nih.gov/ij).

2.10 Immunoprecipitation

Immunoprecipitation was performed in order to detect the interaction between Hsp60 and PGC1α in C2C12 cells transfected with pCMV6-Entry-HSPD1. Briefly, 500 μg of protein from total cells lysates were incubated with the primary antibody (rabbit polyclonal anti-HSP60, H-300, sc-13966, Santa Cruz Biotechnology) overnight at 4 ºC with gentle rotation.

The complexes formed were immunoprecipitated with antibodies linked to Sepharose A beads (GE Healthcare, Milano, Italy) and then, they were revealed by 10% SDS-PAGE using anti-PGC1α primary antibody (diluted, 1:1,000, mouse monoclonal antibody ST1202, Calbiochem). Nonspecifically bound proteins were removed by repeated washings with isotonic lysis buffer.

2.11 Histological analysis

Muscles were fixed in a solution of acetone, methanol and water (2:2:1) for 12 hours, washed in tap water and dehydrated with ethanol at 70, 96, 100% v/v. After dehydration, the tissue pieces were placed in xylol for 1.5 hours and embedded into paraffin. The embedded muscles were sliced into sections (5 μm) that were mounted on glass slides.

These sections were subjected a deparaffination protocol before any analysis. This protocol consists of an alcohols decreasing scale that rehydrate sections preparing them to receive the following treatments.

Chambers slides with muscle cells, after a PBS washing were fixed in ice methanol for 30 minutes at room temperature (RT).

2.11.1 Immunohistochemistry

For immunohistochemical analysis, the deparaffinated serial sections were incubated in an "antigen unmasking solution" (10 mM tri-sodium citrate, 0.05% Tween-20) for 10 min at 75°C, after they were processed by the MACH1 kit (M1u539g, Biocare, USA), used according to the manufacturer's instructions.

The sections were incubated in primary antibodies, including anti-myosin heavy chain-I (MHC-I, A4951, Hybridoma Bank, USA), anti-myosin heavy chain-II (MHC-II, A474, Hybridoma Bank, USA) and anti-Hsp60 (rabbit polyclonal antibody ab53109, Abcam, UK), in a humidified chamber overnight at 4°C. The following day, the sections were incubated for 1 hour with the secondary antibody and polymers as previously described (23592297). Finally, the slides were coverslipped, and images were captured using a Leica DM5000 upright microscope (Leica Microsystems, Heidelberg, Germany).

The cross-sectional area (CSA) of the type I muscle fibres of the posterior muscle group from the hindlimbs was measured using ImageJ 1.41 software to evaluate the

effect of endurance training. The analyses were performed using 5 fields per section, 5 sections per mice (40 μm between sections) and 8 mice per group.

Densitometric analysis of the staining intensity of the anti-Hsp60 antibody was performed using ImageJ 1.41 software. The acquired image (RGB) was transformed to greyscale (32-bit) and then inverted. In the 0-255 greyscale image, 0 corresponds to no positivity and 255 corresponds to maximum positivity the staining intensity of each measured fibre was expressed as the pixel intensity (PI) normalized to that of the CSA.

2.11.2 Immunofluorescence

For immunofluorescence, deparaffinized sections and fixed cells were incubated in the "antigen unmasking solution" (10 mM tri-sodium citrate, 0.05% Tween-20) for 10 min at 75°C or RT respectively and treated with a blocking solution (3% BSA in PBS) for 30 min.

Next, the primary antibody (anti-Hsp60, rabbit polyclonal ab53109, Abcam; anti-MHC-I, mouse monoclonal A4.74, Hybridoma Bank; anti-PGC1α, mouse monoclonal ST1202, Calbiochem; anti-laminin, rabbit polyclonal AB2034, Millipore, USA; anti-DDK, mouse monoclonal TA5001, Origene, USA) diluted 1:50, was applied, and the sections were incubated in a humidified chamber overnight at 4°C. Then, the sections were incubated for 1 hour at RT with a conjugated secondary antibody (anti-rabbit IgG–FITC antibody produced in goat, F0382, Sigma-Aldrich; anti-mouse IgG-TRITC antibody produced in goat, T5393, Sigma-Aldrich). Nucleus were stained with Hoescht Stain Solution (1:1000, Hoechst 33258, Sigma-Aldrich, Germany).

The slides were treated with PermaFluor Mountant (Thermo Fisher Scientific Inc.) and cover slipped. The images were captured using a Leica DM5000 upright microscope (Leica Microsystems, Heidelberg, Germany) or a Leica Confocal Microscope TCS SP8 (Leica Microsystems).

2.12 ELISA: enzyme-linked immunoadsorbent assay

Polyvinylchloride microtiter plates (High bond cod. 353279, BD Biosciences San Jose, CA, USA) were coated with H-300, rabbit polyclonal antibody raised against amino acids 274-573 mapping at the C-terminus of Hsp60 of human origin (H-300, sc-13966, Santa Cruz Biotechnology) 10 μg/ml in PBS (phosphate buffered saline), 50 μl/well, overnight at 4°C.

After, the plates were blocked with 3% BSA in PBS (200 µl/well, 2h at RT). All subsequent steps were carried out at RT.

It was added the 2° element (that will stick to the coating) in PBS/ 1%BSA, 50µl x well: standard curve for Hsp60 (180ng/ml), (diluted 1:25; 1:12.5; 1:6.25; 1:3.12); conditioned medium of C2C12-NT, C2C12-pcMV6-Hsd1, C2C12-pcDNA-mok.

Washed 4 times with PBS and treated with AbI anti-Hsp60-ms (k19, sc-1722, Santa Cruz Biotechnology) 10µg/ml in PBS/ 1%BSA 1h (R.T.), 50µl x; washed 4 times with PBS, again. After, 50µl x well of AbII HPRT-ms 1:1000 in PBS/ 1%BSA 1h (R.T.) was putted in. After the final wash, the plates were incubated with 0.4 mg/ml o-phenylenediamine (OPD: P-8287, Sigma-Aldrich) solution in 7.5ml of distilled water, with 10ul of hydrogen peroxide 36%; 100 µl/well, 30 min. The reaction was stopped by adding 10% (v/v) sulfuric acid (100 µl/well), and the absorbance of each well was read at 490 nm. Serum concentrations (in ng/ml) of Hsp60 was calculated according to the standard curves obtained by using recombinant human Hsp60 (V13-31176, Vinci-Biochem srl, Firenze, Italy) in the sandwich ELISA.

2.13 Statistical analyses

Body weight and force data were statistically analysed via two-way ANOVA for repeated measurements, while all the other data were analysed via one-way ANOVA for single measurements. If a significant difference was detected during ANOVA analyses, this was further evaluated by Bonferroni post-hoc test. All statistical analyses were performed using GraphPad Prism^{TM} 4.0 software (GraphPad Software Inc., San Diego, California, USA). All data are presented as the means ± SD, and the level of statistical significance was set at $p<0.05$.

3 RESULTS

3.1 Functional effects of endurance exercise

The mice from both groups, sedentary (SED) and trained (TR) were weighed at the beginning of the experiment and after every two weeks.

They showed a significant increase in body weight during the 45 days of experimentation (P<0.001). Trained groups for 30 and 45 days (TR30 and TR45, respectively) and sedentary groups for 30 and 45 days (SED30 and SED45, respectively) showed a significant increase in the body weight compared to trained groups for 15 days (TR15) and sedentary groups for 15 days (SED15), respectively (P<0.001); while the body weight of TR45 and SED45 mice increased significantly compared to TR30 and SED30 mice, respectively (P<0.001).

Moreover, only the mice trained for 45 days underwent a reduced increase in body weight compared to the corresponding sedentary mice (P<0.05) (Fig. 6a).

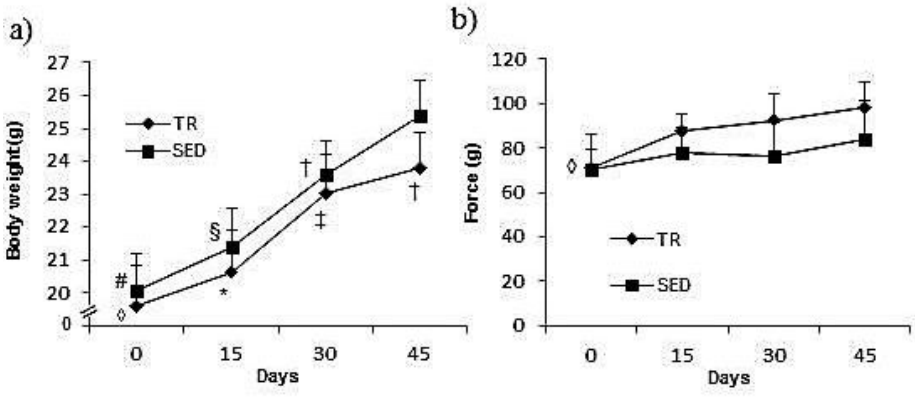

Fig. 1
Functional effects of endurance exercise on the body weight, strength, . a), changes in the body weight over time. Square (■) sedentary (SED) mice; Rhombus (◆) trained (TR) mice; horizontal axis, time of training. Data are presented as the means ± SD. # 34 significantly different from SED15 (n=8), SED30 (n=8) and SED45 (n=8) mice (P<0.001); * significantly different than TR30 (n=8) and TR45 (n=8) mice (P<0.001); § significantly different from SED30 and SED45 mice (P<0.001); ‡ significantly different from TR45 mice (P<0.001); † significantly different from SED45 mice (P<0.05). b), strength of the forelimbs. Square (■) SED mice; Rhombus (◆) TR mice; horizontal axis, time of training. Data are presented as the means ± SD. ◊ significantly different from TR15 (n=8), TR30 and TR45 (P<0.001).

The strength of the mice and the cross section area (CSA) of the type I muscle fibres were measured. The strength results revealed significant increases for the trained groups after 15, 30, and 45 days (P<0.001), while no significant differences were detected in the sedentary groups (Fig. 6b). Moreover, morphometric analysis revealed a

significant increase in the CSA of the type I fibres in TR45 mice compared to the TR15 mice (P<0.001) (Fig. 7).

These increases in the strength of the mice and CSA of the type I muscle fibres confirm that endurance training induced significant modifications and adaptations in skeletal muscle improving muscular fitness

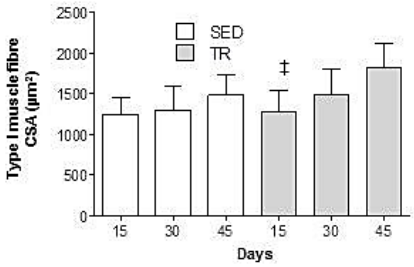

Fig. 2
Functional effects of endurance exercise on Cross section Area (CSA). Histogram showing the results for the CSA of type I fibres of the posterior group of hindlimb muscles. An average of 435 fibres was analyzed for each mouse. Bars, groups of mice; open bars, SED mice; shaded bars, TR mice; horizontal axis, time of training. ‡ significantly different from 45-TR.

3.2 Hsp60 and fibres type in posterior muscle group of mouse hindlimbs

To evaluate Hsp60 levels in each muscle of the posterior group of hindlimb, the cross-sections of the entire muscle group were analyzed by immunohistochemistry. In the same analysis was observed both Hsp60 and fibres type content on serial cross-sections.

The expression of Hsp60 resulted inhomogeneous between the three muscles (Fig. 8aI). In *soleus* all of muscle fibres were positive and in *plantaris* only approximately 55% of the fibres. While, only the red area of *gastrocnemius* was positive to Hsp60; the deeper region in lateral and medial regions to the *plantaris*.

The A4951 and the A474 antibody were used to detect MHC-I (Fig. 8aII/bII) and MHC-IIa/IIx (8aIII/bIII) respectively. By examining overlapping serial cross-sections of the same sample stained for MHC-I and MHC-IIa/x, it was possible to identify type IIb fibres because they were unstained. Type I fibres resulted more abundant in the *soleus*; on the contrary type IIa and IIx fibres were more present in the *plantaris* and the *gastrocnemius* muscles.

Concerning distribution of Hsp60 protein, in different fibres type, it showed a mosaic-staining pattern (Fig. 8bI).

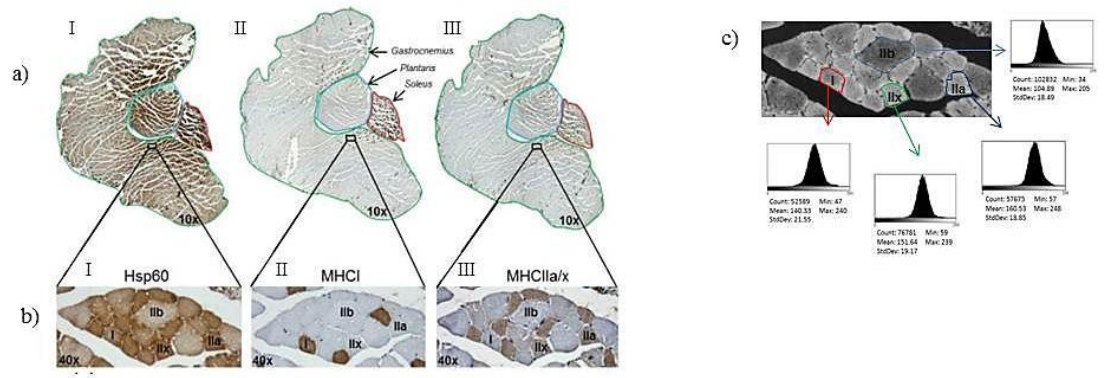

Fig. 3
a), immunohistochemistry for Hsp60 (I), MHC-I (II) and MHC-IIa/x (III) in serial cross-sections of the posterior group of hindlimb muscles, reconstructed by combining multiple images captured at low magnification (10x) (*gastrocnemius*, *soleus*, and *plantaris*, are circled in green, red, and blue, respectively). b), enhanced magnification of the images shown in a). Type IIb fibres are negative to antibodies anti-MHC-I and anti-MHCIIa/x. Bar 25 µm. c), representative images used for densitometric analysis of the staining intensity of a cross-section immunostained for Hsp60. The analysis was performed using 5 fields per section, 5 sections per mice (40 µm between sections) and 8 mice per group. An average of 435 fibres was analyzed for each mouse. The acquired RGB image (Bb) was transformed to a greyscale image (32-bit) and then inverted. Representative histograms of the fibres I, IIa, IIb, and IIx are shown in the small framed panels, where 0 corresponds to no positivity and 255 corresponds to maximal positivity.

The levels of Hsp60 in each muscle fibre type were analyzed only at 45 days because the overall greatest changes were detected at this time point.

Densitometric analysis (Fig. 8c) of serial cross-sections of muscle from sedentary mice (SED45), analyzed by immunohistochemistry, revealed that the Hsp60 protein was more elevated in type IIa fibres and below, in decreasing quantity, in type I fibres (P<0.05) and in type IIx fibres (P<0.05). Type IIb fibres displayed lower levels of Hsp60 than any other fibre type (P<0.05).

Again, quantification of staining intensity (Fig. 9) let on that endurance exercise training induced a significant increase in type I fibres in the *gastrocnemius* (Fig.9a/c) and the *soleus* of trained mice compared to sedentary mice at 45 days (P<0.01).

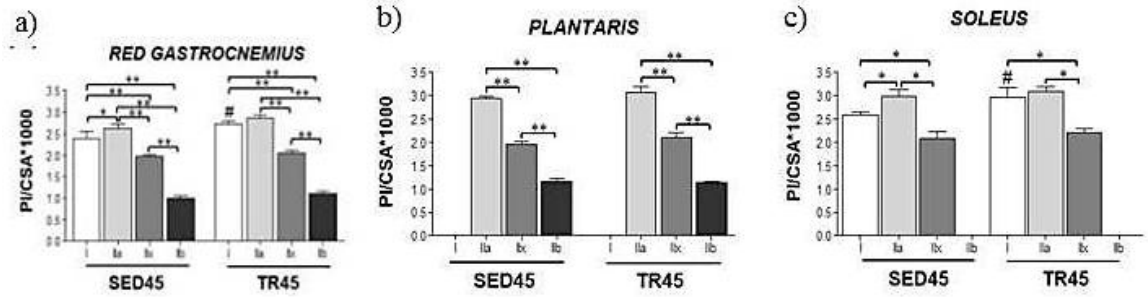

Fig. 4
Staining intensity (determined with ImageJ 1.41 software) of the fibres. It was expressed as the mean pixel intensity (PI) normalized to the cross-sectional area (CSA) for the red *gastrocnemius* (a), the *plantaris* (b), and the *soleus* (c). SED45 and TR45 indicate trained and sedentary mice on day 45, respectively. Data are presented as the means ± SD. # significantly different from type I fibres from SED45 mice (P<0.01), * (P<0.05), ** (P<0.001).

3.3 Hsp60 levels after endurance training

The mosaic staining pattern displayed with immunohistochemistry (in Fig. 8bI), and the increase in type I fibres in TR45 mice compared to the control (Fig.9) was also demonstrated by confocal microscopy. Also, this showed an increase in Hsp60 level in trained mice rather than in sedentary.

by the double fluorescence method type I fibres were stained with anti-MHC-I (Fig. 10aII/V) and anti Hsp60 (Fig. 10aI/IV) antibody, then the content of Hsp60 for each fibre was determined, using the Leica application suite advanced fluorescences software; excluding the interstitial cells.

Type I fibres were strongly positive for the Hsp60 staining, and there was a significant higher level of this protein in trained than in sedentary mice ($P<0.05$) (Fig. 10b).

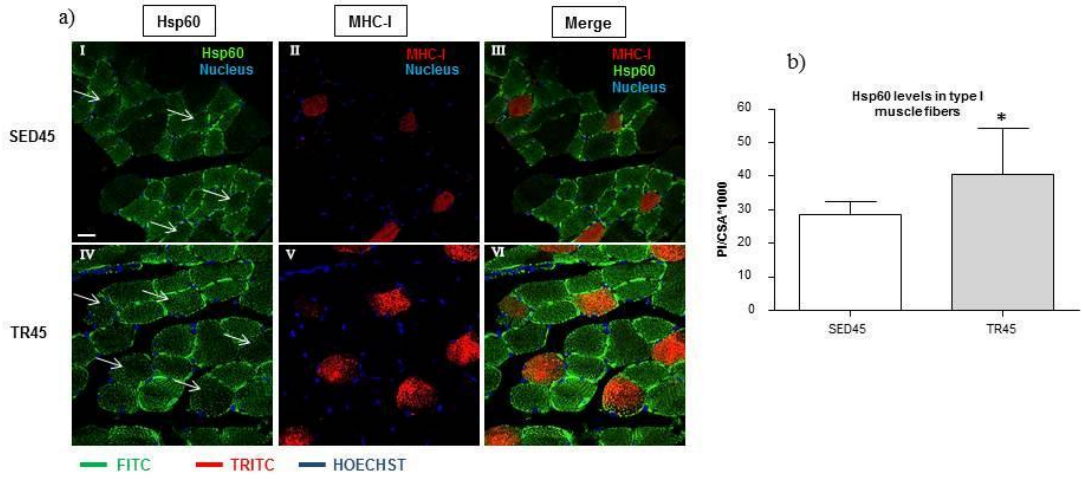

Fig. 5
Confocal microscopy analysis further demonstrates that Hsp60 protein levels increase in mice trained for 45 days. a), immunofluorescence for Hsp60 and MHC-I of cross-sections of sedentary and trained mice at 45 days (SED45, n=8, and TR45, n=8, respectively); the arrows indicate the type I fibres. Bar 25 µm. b), the staining intensity for Hsp60 (bars) of type I fibres was expressed as the mean pixel intensity (PI) normalized to the CSA (cross-sectional area) using the software Leica application suite advanced fluorescences software. Open bar, sedentary (SED45) mice; shaded bar, trained (TR45) mice; both on day 45. Data are presented as the means ± SD. * significantly different from SED45 mice (P<0.05).

In immunofluorescence images it was evident that Hsp60 was present both in the interstitial cells and inside the fibres (Fig. 11a). It was localized inter-myofibrillar (IMF) mitochondria like positive spots inside myofibrils, but also in sub-sarcolemmal (SS) mitochondria as positive bundles beneath the plasma membrane and (Fig. 11b).

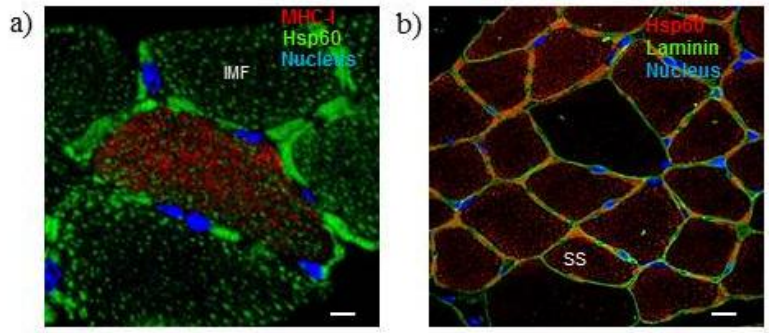

Fig. 6
a), representative immunofluorescence image revealing that Hsp60 was localized also in inter-myofibrillar mitochondria (IMF). Bar 10 µm. b), representative immunofluorescence image revealing that Hsp60 was localized to the subsarcolemmal (SS) space. Bar 20 µm.

Then, considering that many fibres positive for Hsp60 were detected in *soleus* and it is richer in type I, IIa, and IIx fibres compared to other posterior muscles, the attention focused about this muscle. This analysis revealed that endurance exercise had a positive effect on Hsp60 protein levels (Fig. 12a), it showed a significant increase in the trained mice compared to the sedentary mice. A significant difference was detected between the TR30 and SED30 mice ($P<0.05$) and the TR45 and SED45 mice ($P<0.001$) (Fig. 12b).

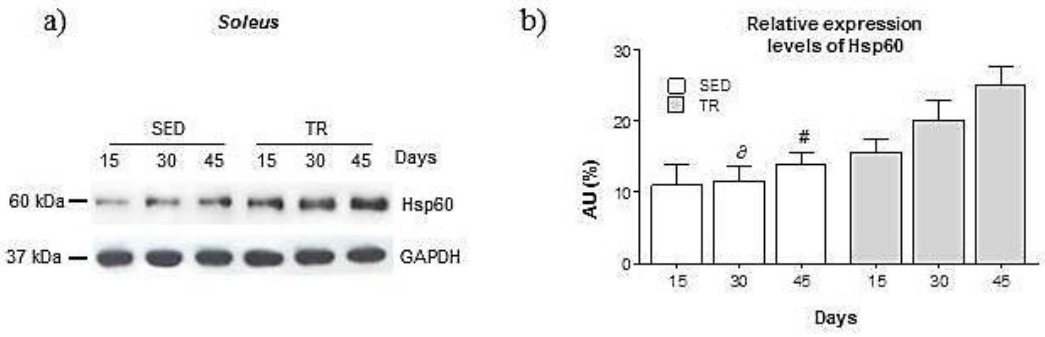

Fig. 7
a), representative western blots of Hsp60 (60 kDa) in the *soleus* from the trained (n=8) and sedentary mice (n=8) at various time points. 40µg of protein was loaded in each lane; GAPDH (37 kDa) was used as the loading control. B), relative expression levels of Hsp60 in the *soleus*. Open bars, sedentary mice; shaded bars, trained mice; horizontal axis, days. AU: Arbitrary Unit. ∂ significantly different from TR30 mice (P<0.05). # significantly different from TR45 mice (P<0.001).

This result was furthermore confirmation by qRT-PCR analysis, that reported a significant increase in Hsp60 transcript (Fig. 13) in *soleus* muscle of TR45 compared to SED45 ones.

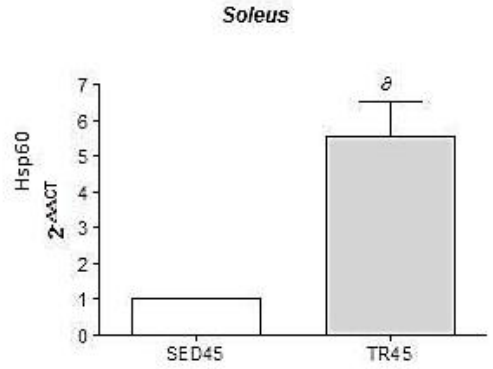

Fig. 8
qRT-PCR analysis of *hsp60* gene in the *soleus*. Bars show the *hsp60* gene expression levels normalized for the reference genes, according to the Livak Method (2-ΔΔCT) (Schmittgen and Livak, 2008) in *soleus* of sedentary (n=6) and trained (n=6) mice at 45 days (SED45, and TR45, respectively. ∂ significantly different from SED45 (P<0.01);

Concurrently to the increases in Hsp60 levels in muscle, ELISA test revealed blood Hsp60 levels of trained mice higher than sedentary mice at 30 and 45 days (Fig. 14).

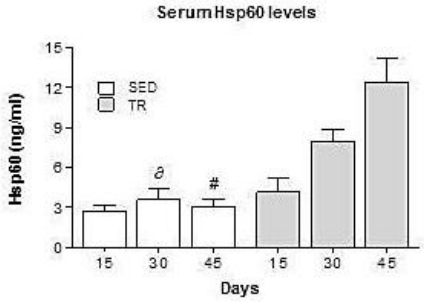

Fig. 9
Serum levels of Hsp60 in SED (n=8) and TR (n=8) groups at various time points. Open bars, sedentary (SED) mice; shaded bars, trained (TR) mice; horizontal axis, days. Data are presented as the means ± SD. ∂ significantly different from TR30 mice (P<0.05). # significantly different from TR45 mice (P<0.001).

3.4 Mitochondrial biogenesis

Generally, Hsp60 is considered a biomarker of mitochondria content, considering its most common location. Then, it was interesting to investigate if the increase in the levels of Hsp60 was accompanied by an increase in the number of mitochondria.

That was valuated through qRT-PCR. with a protocols that compare the copy number of mitochondrial genes, to the nuclear ones. Indeed, as expected, TR45 mice showed more than double of mitochondria compared to SED45 (Fig. 15).

Then, the increase in Hsp60 protein and gene levels was correlated to an increase in mitochondrial DNA.

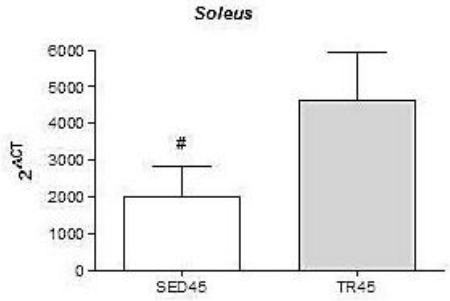

Fig. 10
Copy number of mitochondrial genes in the *soleus* of sedentary mice (n=6) at day 45 (SED45, open bar) and trained mice (n=6) at day 45 (TR45, shaded bar). # different from 45 TR p<0.001.

3.5 Transfection efficacy

It was realized a closed cell system where to observe the effects of Hsp60 protein overexpressed, without any physiological interference as could occur in vivo. To do this was employed a myoblasts cell line called C2C12. Then, part of C2C12 cells was transfected with pCMV6-Entry-HSD1 plasmid that contained the sequence defining overexpression of Hsp60,and a little oligonucleotide coding for DDK, used like a tag to detect really transfected cells. Simultaneously other plates of C2C12 was transfected with pcDNA 3.1 like negative control plasmid. Again, others C2C12 were processed with silencer pre-designed siRNA against *Hsp60* and its siRNA negative control, to examine the effects of absence of the protein.

The working of protocol was confirmed by confocal analysis. Expression of Hsp60 and DDK (Fig. 16a) and knock down of *Hsp60* performed by RNA interference (Fig. 16b) were visible through immunofluorescence analysis.

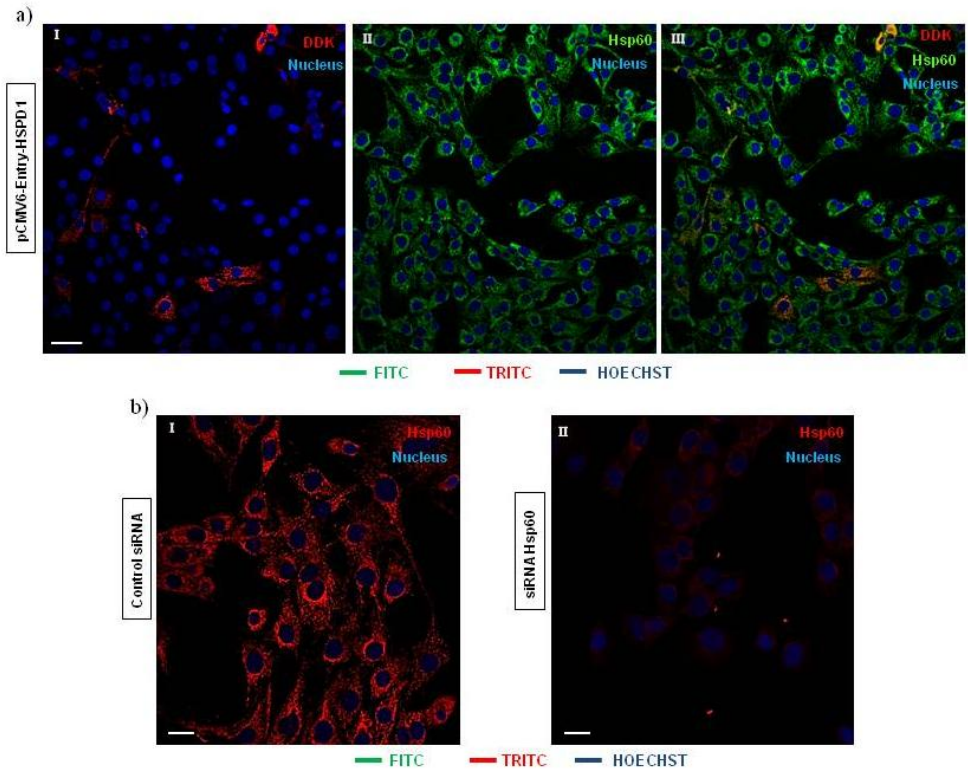

Fig. 11
a), immunofluorescence images of C2C12 myoblasts cell line transfected with pCMV6-Entry-HSPD1 vector, (pcDNA3.1 was used as a negative control), the expression of the tag DDK demonstrated the efficiency of transfection of these cells (Bar 50 µm); b), immunofluorescence images of C2C12 myoblasts treated with Hsp60 siRNA (siRNA Hsp60) (Bar 25 µm).

Further confirmation that transfection protocol worked we performed a qRT-PCR with RNA extracted by transfected and silenced cells (Fig. 17). We found that the *hsp60* gene was considerably more expressed in pCMV6-Entry-HSD1 cells than in pcDNA and siRNA cells. This increase was comparable to that verified in *soleus* of TR45 compared to SED45 (Fig. 13). So we proposed that the increase in Hsp60 protein levels following endurance training, was due, at least in part, to a physiological increase in *hsp60* gene

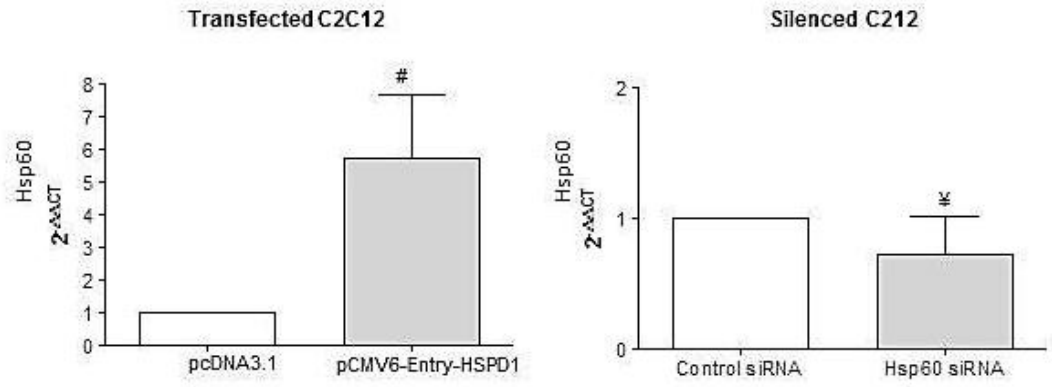

Fig. 12
qRT-PCR analysis of *hsp60* gene in transfected C2C12 cells. Bars show the *hsp60* gene expression levels normalized for the reference genes, according to the Livak Method (2-ΔΔCT) (Schmittgen and Livak, 2008) in C2C12 myoblasts transfected with pCMV6-Entry-HSPD1 vector to over-express *hsp60* (pcDNA3.1 was used as a negative control); and Hsp60 siRNA for silencing Hsp60 (scramble siRNA used as a negative control, Control siRNA). # significantly different from pcDNA3.1 (P<0.01); ¥ significantly different from Control siRNA.

In spite of this, in transfected cells, there wasn't the increase in the number of mitochondria like in muscle fibres of trained mice, as demonstrated by the levels of mtDNA copy number(Fig. 18).

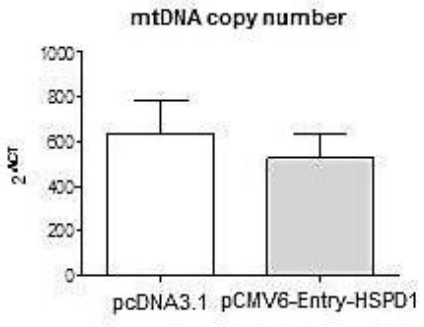

Fig. 13
Copy number of mitochondrial genes in C2C12 myoblast transfected with pCMV6-Entry-HSPD1 vector (shaded bar) (pcDNA3.1 was used as a negative control, open bar).

3.6 PGC1α in Hsp60 overexpressed models

Therefore, the interest of the experimental study moved on PGC1α that, for literature, is the protagonist of mitochondrial biogenesis mechanism.

Western blotting (Fig. 19) showed an increase in PGC1α in mouse muscle, induced by endurance training, similar to that observed in C2C12 cells transfected with pCMV6-Entry-HSPD1.

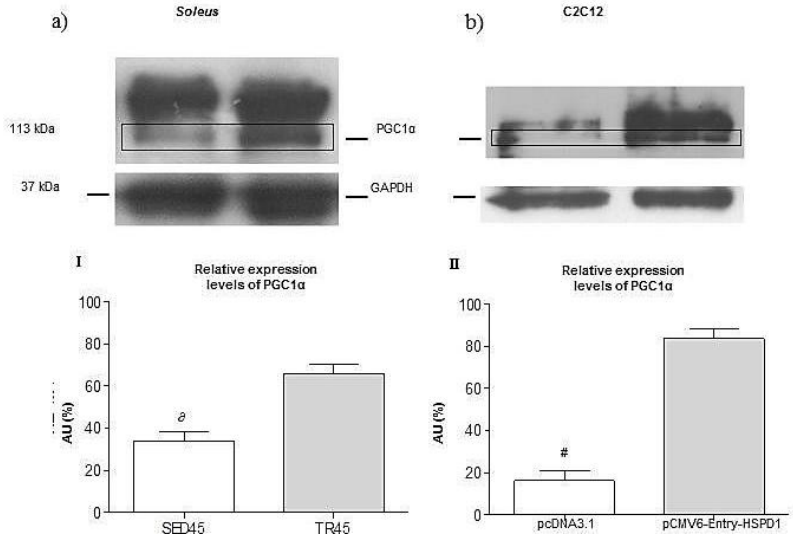

Fig. 14
Representative western blots of PGC1 α1 levels in the *soleus* (a) of trained and sedentary mice, and in C2C12 cells (b) upon transfection with pCMV-Entry-HSPD1 vector (pcDNA3.1 was used as a negative control). Relative expression levels (I, II) (bars) of PGC1 α1 (113 kDa). ∂ significantly different from TR45 p<0.001; # different from pCMV6-Entry-Hspd1 p<0.0001.

So, we decided to evaluate also the gene expression levels of the co-activator PGC1α in its isoforms suggested as involved in exercise training (Ruas JL et al., 2012). It was examined PGC1α in its total form, PGC1 α1 the transcript originating from the proximal promoter corresponding to a 113 kDa protein; α2 the transcript originating from the distal promoter and corresponding to a 41.9 kDa protein; α3 the transcript originating from the alternative distal promoter and corresponding to a 41.0 kDa protein; and α4 the transcript originating from the distal promoter, corresponding to a 29.1 kDa protein, which has undergone an alternative splicing between the 6 and 7 exons.

In the *soleus* of trained mice the PGC1α isoform α4 was not detected but there was an increase in total PGC1α, and in the α1, α2, and α3 isoforms (Fig. 20a), in parallel with the increase in *hsp60* gene expression (Fig. 13 and 17). In C2C12 myoblasts transfected with pCMV6-Entry-HSPD1 we found increase in the expression of PGC1α isoform 1 (Fig. 20b). While the siRNA against *hsp60* did not have any effect on the basal levels of PGC1 α1(Fig. 20b).

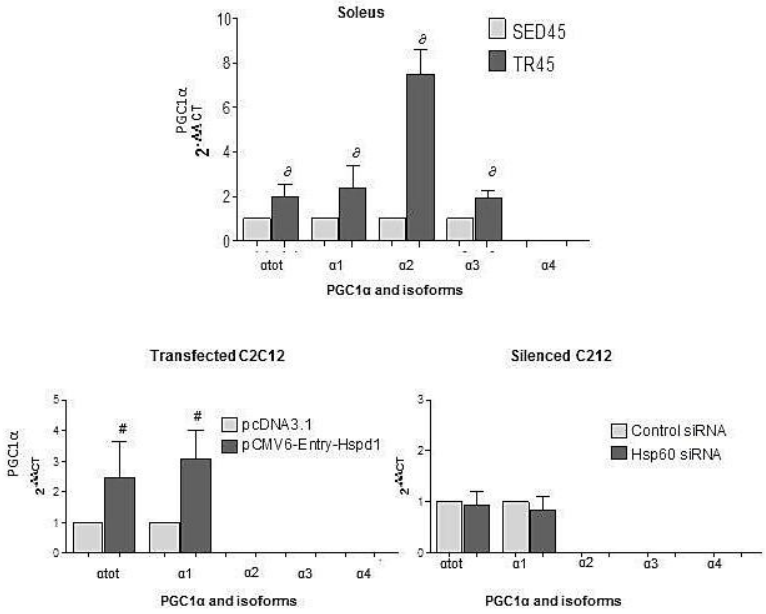

Fig. 15
qRT-PCR analysis of *PGC1α* gene and its isoforms in the *soleus* of trained mice and transfected C2C12 cells. Bars show the PGC1α isoforms [PGC1α total (αtot), isoform 1 (α1), 2 (α2), 3 (α3), 4 (α4)] gene expression normalized for the reference genes, according to the Livak Method (2- ΔΔCT), in: *soleus* of SED45 (grey bars) and TR45 (black bars); C2C12 myoblast transfected with pCMV6-Entry-HSPD1 vector to over-express *hsp60* (pcDNA3.1 was used as a negative control); and Hsp60 siRNA for silencing Hsp60 (scramble siRNA used as a negative control, Control siRNA). Data are presented as means ± SD, bars show the PGC1α isoforms [*PGC1α* total (P<0.01); ∂ significantly different from SED45 (P<0.01); # significantly different from pcDNA3.1 (P<0.01).

We found that elevated levels of Hsp60 protein and expression of the *hsp60* gene were accompanied by an increase in the expression of *PGC1α* gene, both *in vivo* and *in vitro*. These observations suggested that Hsp60 levels and *PGC1α* gene expression were linked in some way.

This hypothesis was strengthened by double immunofluorescence for Hsp60 and PGC1α on sections of SED45 (Fig. 21a) and TR45 (Fig. 21b), which showed again correspondence between increase of Hsp60 and PGC1α protein. In the same slides, with greater magnification, Hsp60 appeared at high levels also in interstitial cells and PGC1α was localized in a cytoplasmic compartment between the nucleus and mitochondria (Fig. 21c). Thanks to the signal of laminin was even more obvious that PGC1α resulted localized in the cytoplasm of interstitial cells (mesenchymal progenitors, connective tissue cells or pericytes) (Fig. 21d).

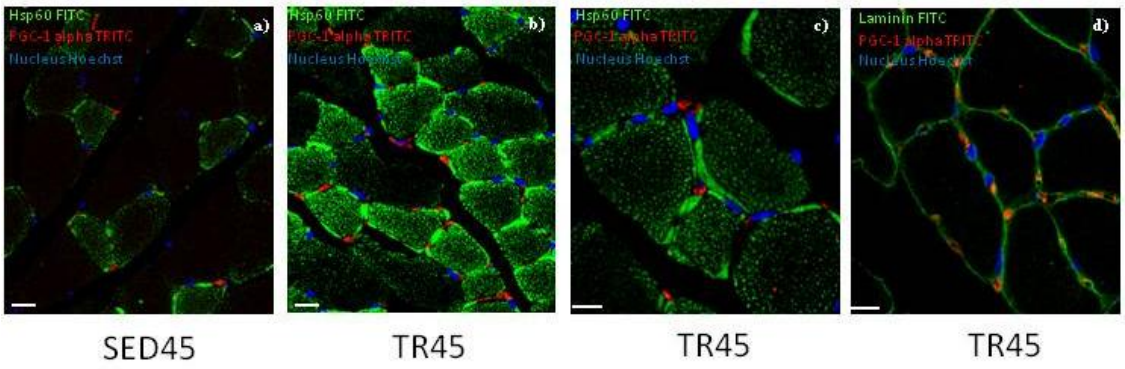

Fig. 16
The confocal microscopy analysis shows the localization of PGC1α positive cells in the skeletal muscle tissue. Immunofluorescence for Hsp60 and PGC1α of muscle cross-sections of sedentary (a) and trained (b) mice at 45 days (SED45 and TR45, respectively). Bar 25 µm. Immunofluorescence for Hsp60 and PGC1α (c) of muscle cross-sections of trained mice at 45 days (TR45) at higher magnification; for laminin and PGC1α (d) that result localized in the interstitial space, outside the fibres;. Bar 15 µm.

Validated a concomitance between overexpression of Hsp60 and the activation of PGC1 α1, it was proper to understand if possible a direct interaction between the two proteins, considering that PGC1α protein is also a transcription factor for it self gene.

For this reason, we have immunoprecipitated Hsp60, of transfected C2C12 samples, and performed a Western blotting analysis on the immunoprecipitation with the anti-PGC1α antibody. The result showed that at 113 kDa PGC1α isoform co-immunoprecipitated with Hsp60 (Fig. 22).

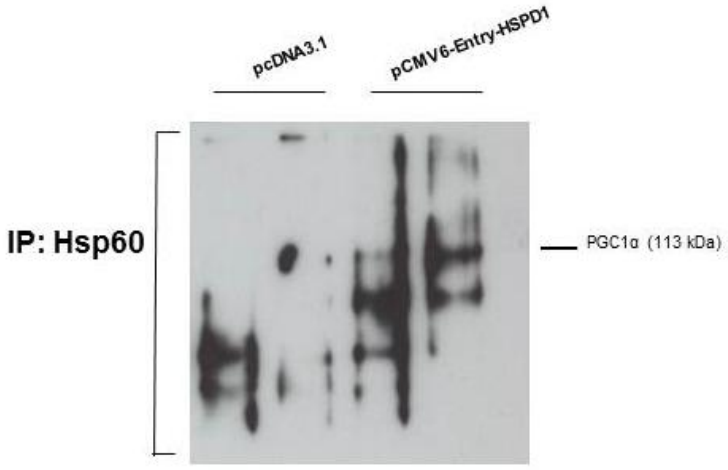

Fig. 17
Representative blot of immunoprecipitation experiments in C2C12 myoblasts transfected with pCMV6-Entry-HSPD1 vector to over-express *hsp60* (pcDNA3.1 was used as a negative control) showing a 113 kDa band corresponding to PGC1α that co-immunoprecipited with Hsp60.

Within of stress response they were also evaluated the protein levels of 4 Hydroxynonenal (4 HNE), manganese superoxide dismutase (Mn SOD), phospho AMP-activated protein kinase alpha1 (p-AMPKα), AMPKα1, AMPKα2 and

Transcription Factor A Mitochondrial (TFAM) both in the muscle of trained mice and in C2C12 cells transfected with pCMV6-Entry-HSPD1.

In *Soleus* muscle, only 4 HNE and p-AMPK presented a significant increase in trained mice, while in transfected C2C12 there was no increase (Fig. 23).

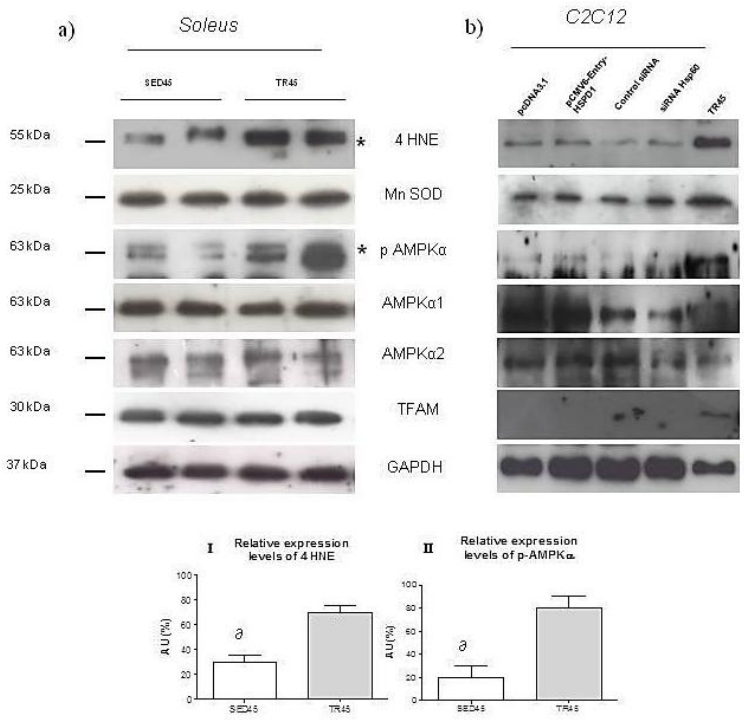

Fig. 18
Representative western blots of 4 HNE (55 kDa), Mn SOD (25 kDa), p-AMPKα (63 kDa), AMPKα1 (63 kDa), AMPKα2 (63 kDa), TFAM (30 kDa) in soleus (a) of sedentary (SED45, open bar, n=8) and trained (TR45, shaded bar, n=8) mice at 45 days, and in transfected C2C12 cells (b). GAPDH (37 kDa) was used as the loading control. Relative expression levels (bars) of 4 HNE (55 kDa) (I) and p-AMPKα (63 kDa) (II). Data are presented as the means ± SD. ∂ significantly different from TR45 mice (P<0.001). AU: Arbitrary Unit.

So the important relation between effects of exercise training and activated molecular pathways in muscles, involved only Hsp60 and PGC1α.

3.7 Paracrine effect of Hsp60

As already demonstrated above (Fig. 14), the endurance training also determined a release of Hsp60 in the bloodstream. Therefore, we wanted to verify if Hsp60 released could have an effect on surrounding elements.

For this purpose we used the closed cells system, C2C12 cells were transfected whit pCMV6-Entry-HSD1 and pcDNA 3.1 plasmids as in previous experiment (Fig. 16). After 48h their conditioned medium was taken, a little part of it was analyzed by

ELISA test and the remaining part was given to different wells of naive C2C12 for 0h, 6h, 12h, 24h, 48h.

The ELISA test (Fig. 24) about conditioned medium confirmed that C2C12 transfected with the pCMV6-Entry-HSPD1 plasmid released more Hsp60, while they were silenced by siRNA against *Hsp60*, they released less protein in extracellular environment.

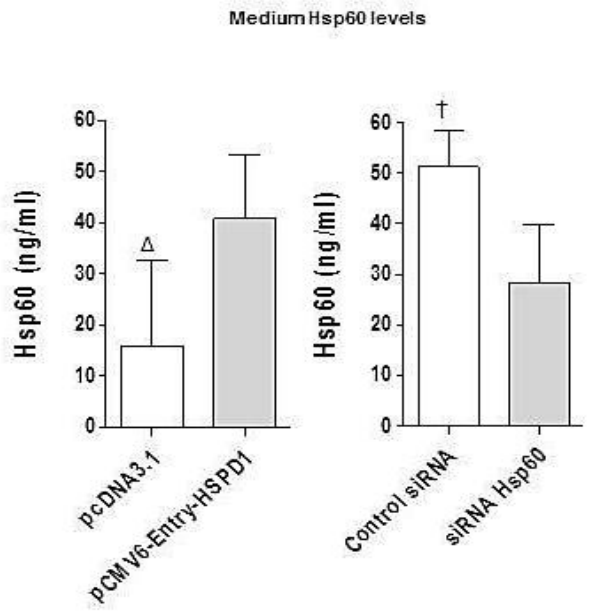

Fig. 19
Medium levels of Hsp60 in C2C12 cells transfected with pCMV6-Entry-HSPD1 vector to overexpress Hsp60 (pcDNA3.1 used as a negative control); and Hsp60 siRNA for silencing Hsp60 (scramble siRNA used as a negative control, Control siRNA). Data are presented as the means ± SD. Δ significantly different from p-CMV-Entry-HSPD1 (P<0.05). † significantly different from siRNA Hsp60 (P<0.05).

While as regards cells treated with conditioned medium at different time, their RNA was extracted and tested through qRT-PCR. The result most relevant concerned cells treated for 6 h with medium from C2C12 transfected with the pCMV6-Entry-HSPD1 plasmid (Fig. 25): they showed a significant increase in the levels of expression of the PGC1 α1 isoform.

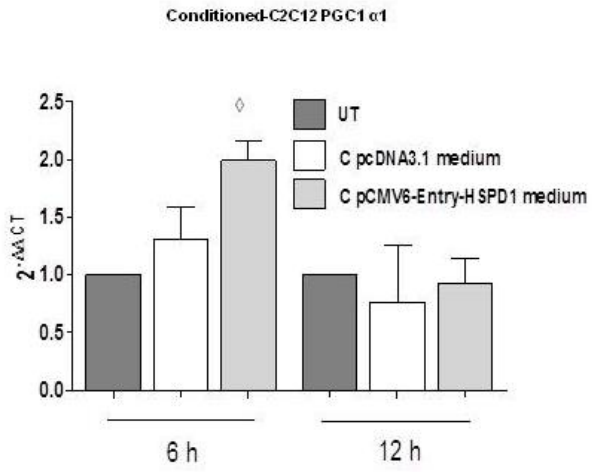

Fig. 20
qRT-PCR analysis of PGC1 α1 isoform in C2C12 cells treated with the conditioned media (Fig. 24) from C2C12 myoblasts transfected with pCMV6-Entry-HSPD1 vector (C pCMV6-Entry-HSPD1) to over-express *hsp60*, and from C2C12 myoblasts transfected with pcDNA3.1 used as a negative control (C pcDNA3.1) for 6 and 12 hours (h). UT: untreated cells. Data are presented as the means ± SD. ◊ significantly different from UT 6 h, C pcDNA3.1 6 h and C pCMV6-Entry-HSPD1 12 h (P<0.01).

High levels of Hsp60 released in the culture medium induced the increase in Hsp60 and PGC1α levels in neighbouring cells.

3.8 Effect of endurance training on cachectic mice

On the basis of these data that confirmed that this trained mouse model defined significant and positive changes in molecular stress response pathways, we undertook a series of experiments applying the endurance training on mice bearing the C26 tumour mass. In all the mice the tumour was visible around 10 days after the inoculation. No differences were present between the groups in the tumour growth delay.

3.8.1 Survival curves

Survival curves of all groups are shown in figure 26. The TR_P protocol conducted after inoculation of C26 not induced a significant increase in the median survival in male and female adult mice (AM-SED/TR_P and AF-SED/TR_P) compared with sedentary groups.

The three different training protocols (TR_L, TR_M and TR_H) completed by adult female mice after 6 weeks of TR_P and tumour inoculation did not induced any significant change in the median survival compared with control mice (AF-SED/SED). While, the adult male mice trained before and after the inoculation (AM-TR_P/TR_L, AM-TR_P/TR_M and AM-TR_P/TR_H) showed an higher median survival than matching adult

female mice (AF-TR_P/TR_L, AF-TR_P/TR_M and AF-TR_P/TR_H, respectively) ($p<0.05$). Moreover the AM-TR_P/TR_M and AM-TR_P/TR_H groups showed an higher median survival than AM-SED/SED group ($p<0.05$).

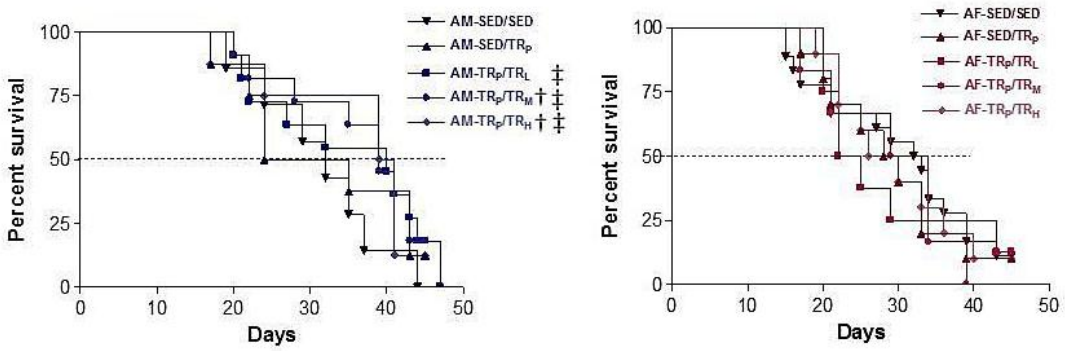

Fig. 21
Surviving curve of male (AM-SED/SED; AM-SED/TRp; AM-TRp/TRl; AM-TRp/TRm; AM-TRp/TRh) and female (AF-SED/SED; AF-SED/TRp; AF-TRp/TRl; AF-TRp/TRm; AF-TRp/TRh) mice groups. † significant different than AM-SED/SED ($p<0.05$); ‡ significant different than corresponding female group ($p<0.05$).

3.8.2 Cachexia curves

Literature defines cachexia as a body weight loss of 15%. In our experimental groups the cachexia occurred around 19 days after tumour inoculation, they showed a similar cachexia curves if expressed in percentage of body weight lost (Fig. 27).

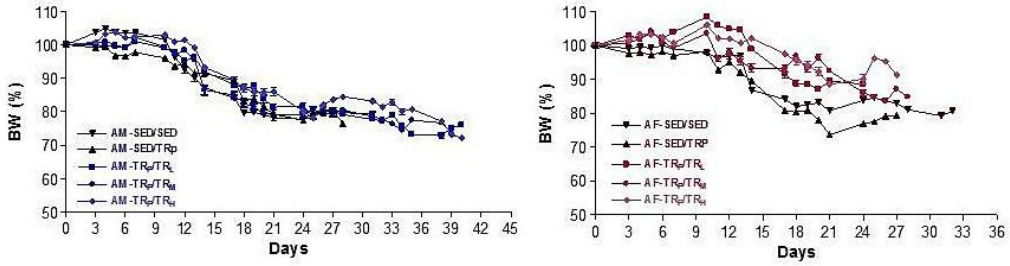

Fig. 22
Representative curve of body weight lost trend in male (AM-SED/SED; AM-SED/TRp; AM-TRp/TRl; AM-TRp/TRm; AM-TRp/TRh) and female (AF-SED/SED; AF-SED/TRp; AF-TRp/TRl; AF-TRp/TRm; AF-TRp/TRh) mice groups.

Only in the AF-TR_P/ TR_H the cachexia occurred significantly later than in AF-SED/SED and AF-SED/TR_P (Table 7).

Moreover, AM-TR_P/TR_M survive longer in a state of cachexia than AF-TRP/ TRM ($p<0.03$), while AM-TR_P/TR_H and AF-SED/TR_P groups survive longer than the AF-TR_P/TR_H group ($p<0.05$).

Groups	Body Weight		Tumor growth delay (d)	Cachexia (d)	Survive in a state of cachexia (d)
	Inoculum (g)	Cachexia (g)			
AM-SED/SED	26.3±1.2	21.3±0.9	11.1±1.1	18.7±2.7	20.0±5.3
AM-SED/ TR_P	26.7±2.0	21.9±2.0	10.7±1.0	17.6±2.9	14.4±10.3
AM-TR_P/ TR_L	26.8±2.0	21.5±2.3	12.2±1.6	20.9±4.5	14.4±8.9
AM-TR_P/ TR_M	26.9±1.6	21.0±2.4	11.4±0.9	21.1±5.6	17.3±9.6 €
AM-TR_P/ TR_H	26.2±1.1	21.7±0.9	10.0±2.1	20.0±3.3	16.1±8.3 $
AF-SED/SED	20.9±1.2	17.4±1.1	10.7±1.3	17.0±4.1 $	13.2±9.5
AF-SED/ TR_P	20.7±1.2	17.3±1.2	10.6±1.2	16.4±2.6 $	14.3±7.8 $
AF-TR_P/ TR_L	18.2±1.0	15.6±0.7	11.4±1.4	19.9±6.1	10.0±7.3
AF-TR_P/ TR_M	19.5±3.1	16.2±2.3	10.8±0.9	20.0±6.5	9.0±5.5
AF-TR_P/ TR_H	19.3±0.8	16.6±0.9	10.5±1.7	22.9±10.3	5.9±4.7

Table 7
Summary of cachexia experiments data for male (AM-SED/SED; AM-SED/TRp; AM-TRp/TRl; AM-TRp/TRm; AM-TRp/TRh) and female AF-SED/SED; AF-SED/TRp; AF-TRp/TRl; AF-TRp/TRm; AF-TRp/TRh) mice groups. € different than AF-TRP/ TRM ($p<0.03$); $ different than AF-TRP/ TRH ($p<0.05$).

4 DISCUSSION

Chronic diseases, cancer, long periods of physics inactivity, malnutrition or aging can cause the establishment of muscle wasting condition characterized by a loss of weight and degeneration of muscle fibres. Muscle wasting involves several molecular pathways promoting protein degradation and interfering with protein synthesis (Eley, Russel, Tisdale, 2007; Eley, Tisdale, 2007; Hasselgren et al., 2002). Products of the catabolism increase oxidative stress inducing the further activation of E3-ub-Li system, the immune response and all the contributing factor to muscle wasting (Li et al., 2003).

The positive effect of exercise training on recovery of lost skeletal muscle mass in muscle wasting condition is well known in literature (Lenk et al., 2012; Bowen et al., 2015). Exercise has the ability to reduce expression of inflammatory cytokines (such as TNFα and IL-6) (Osterziel et al., 1998) and Myostatin, to induce significant phosphorylation on mTOR (Lenk et al., 2012) and to increase the number of adult stem cells in the muscle (Macaluso et al., 2013).

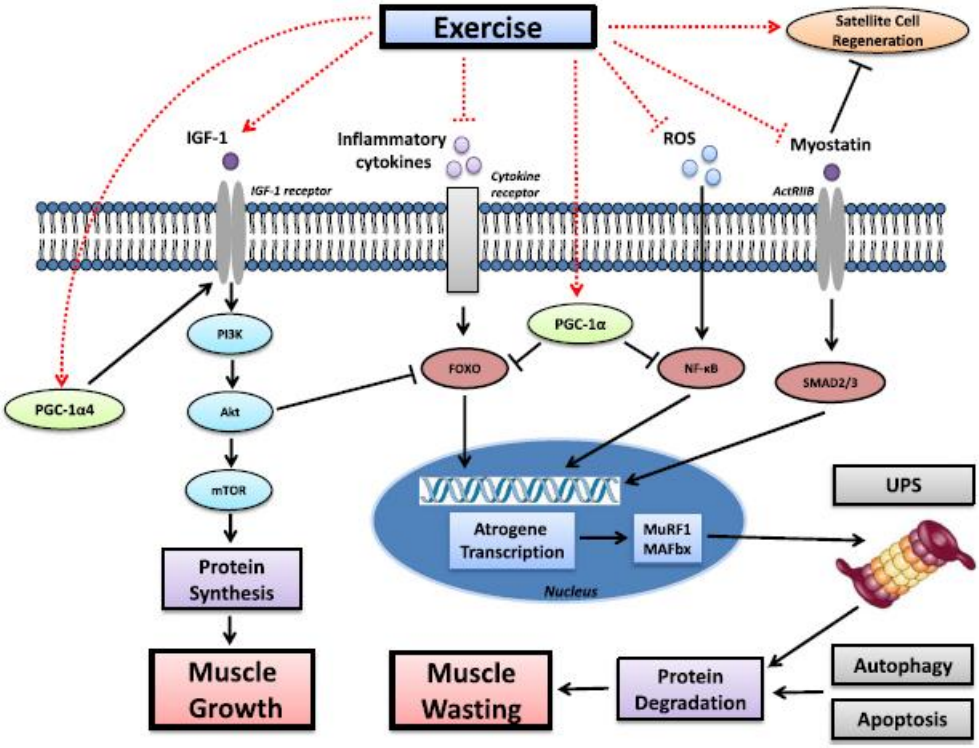

Fig. 23
The effects of exercise on the signalling pathways associated with muscle growth and wasting in sarcopenia and cachexia (Bowen et al., 2015. Skeletal muscle wasting in cachexia and sarcopenia: molecular pathophysiology and impact of exercise training. J Cachexia Sarcopenia Muscle.).

Physical activity generates ROS, but it also stimulates the production of antioxidant enzymes, as superoxide dismutases (SOD) (McArdle, Van Der Meulen et al., 2004) and cyto-protective proteins, like HSPs (McArdle, Dillmann et al., 2004). High levels of ROS and RNS generated by exercise induce muscle adaptations, among which the increase in the cross sectional area of fibres and the increase of mitochondrial biogenesis, key events for the response to stress and muscle regeneration (Atherton et al., 2012).

The endurance protocol used in this study induced a significant loss in body weight, an increase in force and in CSA of muscle fibres in mice, in accordance with the many data published in our laboratory (Di Felice et al., 2007). These changes are considered physiological adaptations due to aerobic training.

The histological analysis of serial muscle cross-sections revealed that Hsp60 immunoreactivity was strongly localized in type I, IIa and IIx muscle fibres, while type IIb muscle fibres appeared only slightly positive for Hsp60 (IIa > I > IIx > IIb). This chaperonin is particularly expressed in *soleus*, *plantaris* and deeper regions of *gastrocnemius*, muscles richest of type I, IIa and IIx muscle fibres.

The fibre-type specific levels of Hsp60 in skeletal muscle is a very novel finding for human and animal model. Very recently, Folkesson et al. (Folkesson et al., 2013) did not detect any fibre type-specific staining of Hsp60 in human, the type I and type II fibres displayed a similarly uniform cytoplasmic staining. Our data appears clearly in contrast with these results, but the same authors indicated that their results were surprising considering that Hsp60 is a molecular chaperone involved in mitochondrial homeostasis (Campanella et al., 2008; Campanella et al., 2009; Di Felice et al., 2005) and given the differences in mitochondrial content between slow and fast fibres (Folkesson et al., 2013). In our opinion, the lack of fibre-type specificity of Hsp60 in Folkesson et al. (Folkesson et al., 2013) may be explained by the quantitative distribution of the fibre types in the muscle. In fact, they examined the vastus lateralis muscle from humans, which is composed almost exclusively of type I and IIa muscle fibres (Bloemberg and Quadrilatero, 2012). However, the discrepancy in the results may be caused by the sample preparation (frozen Vs. acetone/methanol fixation) or antibody specificity (StressGen Vs. Abcam).

Only a few reports have been published describing the levels and the expression of Hsp60 in skeletal muscle of animals at rest or under stress, and their results are contradictory. Mattson et al. (Mattson et al., 2000) demonstrated an increase in Hsp60

expression in the rat after an 8-week training protocol in *plantaris*, but not in *soleus*. Treadmill running induced changes in Hsp60 level in parallel to increases in the activity of citrate synthase, but the authors did not examine cellular localisation or the expression of this protein in each fibre type (Mattson et al., 2000). Despite this, in another study, an increase in Hsp60 level was detected in rat *soleus* muscles after 16-20 weeks of treadmill endurance training (Samelman, 2000). Again, Oishi et al. (Oishi et al., 2003) demonstrated an increase in Hsp60 level in the deep (relatively high percentage of slow fibres) and in superficial regions (only fast fibres) of the *gastrocnemius* after a single bout of heat stress. This increase was similar to that following a prolonged periods of treadmill running (Mattson et al., 2000; Samelman, 2000). Furthermore, the authors found that the level of Hsp60 was different between muscles or muscle regions containing distinct fibre type compositions, suggesting that the fibre type composition of a muscle or muscle region may impact the response of specific HSPs to stress (Oishi et al., 2003).

The results obtained were confirmed also with confocal microscope, Western Blotting and qRT-PCR analysis of *soleus* muscle. Moreover, we detected significant high levels of Hsp60 in serum of trained mice compared to sedentary, using ELISA test.

Upregulation of muscle Hsp60 levels after exercise training was in agreement with findings from other animal studies (Morton et al., 2008 and Mattson et al., 2000). Moreover, in our study, Hsp60 levels increased significantly exclusively in type I fibres of the red *gastrocnemius* and the *soleus*, although Hsp60 content increased by about two folds according to the Western blotting results, while immunohistochemistry showed only a 15% increase in type I fibres; this may be explained as a difference in the experimental approaches. At the best of our knowledge, our study is the first one that analyses the hsp60 gene expression after endurance training. Concerning higher levels of circulating Hsp60, they have been observed in various pathological conditions, such as type 2 diabetes (Yuan et al., 2011), coronary heart disease (Zhang et al., 2008), carotid arterial stiffness (Ellins et al., 2008), physiological and psychosocial stress (Lewthwaite et al., 2002), atherosclerosis (Xu et al., 2000), Hashimoto's thyroiditis (Marino Gammazza et al., 2014), and in normal and aged individuals (Pockley et al., 1999 and Rea et al., 2001), and after a single bout of exercise (Febbraio et al., 2004).

Mitochondrial biogenesis is one of the most studied muscle adaptations following aerobic training. We observed a significant increase in mitochondrial DNA copies in trained mice compared to sedentary. This data were in parallel with the increase of

Hsp60 levels, suggesting that this chaperone might facilitate proteins import and folding during exercise-induced mitochondrial biogenesis. For instance, this could be a protecting mechanism to maintain mitochondrial homeostasis during exercise-induced damage (Morton et al., 2008).

The principal actor of mitochondrial biogenesis is the transcriptional factor PGC1α (Powers et al., 2011 and Arany et al., 2008). We investigated PGC1α isoforms levels after 45 days of endurance exercise and in C2C12 overexpressing Hsp60. In particular, we analysed the PGC1α isoforms transcribed by the activation of the proximal and the alternative promoter, or as a result of an alternative splicing of exon 1 (When et al., 2014). The results obtained showed a significant increase of PGC1α total, α1, α2 and α3 isoform levels in *soleus* muscle of trained mice, while C2C12 cells overexpressing Hsp60 showed a significant increase of PGC1α total and α1 isoform levels. Other studies demonstrated increased levels of isoform α1 compared to isoform α2 in resistance training experiments (Ruas et al., 2012). This discrepancy with our results may be due to a difference in the training protocol used by us, as compared to that applied by the other investigators. Moreover, NT-PGC1α alternative splicing isoforms (NT-PGC1 α-a, b, and c) mRNAs may be induced by a single bout of high, medium, and low intensity exercise (Wen et al., 2014), while in our experiments, using a pan anti-body against all PGC1α isoforms, any 35 kDa band (corresponding to NT-PGC1α isoforms) was found, and we never detected PGC1 α4.

These results indicate that a prolonged endurance exercise causes, predominantly, an increase in the levels PGC1 α1, α2, and, α3 isoforms, with the greatest increase being that of the α2 isoform.

The most interesting result obtained in our study was the correlation between Hsp60 and PGC1α in mice muscles samples and in the cellular one. In trained mice, the interaction was confirmed by double IF in *soleus;* in the cells the immunoprecipitation assay showed the presence of PGC1α together with Hsp60. In the contrary, other proteins usually involved in stress response pathways did not undergo any changes neither *in vitro* nor *in vivo*, except for a significant increase of 4 HNE and p-AMPK in *soleus* of trained mice.

Confocal microscope images showed overexpression of Hsp60 both in muscle fibres and interstitial cells although PGC1α was detectable only in the latter. Our idea was that Hsp60 could have a paracrine action on surrounding elements. This finding suggested further experiments on transfected cells; their medium was used to treat naïve

cells. The transfected cells displayed high levels of Hsp60 released in the medium and the naïve cells treated with this medium showed high PGC1 α1 mRNA levels. Therefore, our hypothesis regarding the paracrine effect of Hsp60 released in the extracellular environment was confirmed *in vivo* on muscle fibres and *in vitro* on transfected cells. In particular, Hsp60 released by the cells might trigger the overexpression of PGC1 α1 in the surrounding cells. The release of Hsp60 may occur via vesicles leading it up to the target represented by interstitial and undifferentiated surrounding cells, where interaction of Hsp60 with PGC1α might promote greater mitochondrial biogenesis, supporting muscle regeneration and recovery in muscle wasting.

In the light of our results and conclusions, we applied exercise training to a pathological condition (cancer cachexia) to observe if the molecular mechanisms arising from our endurance protocol, engaging Hsp60 and mitochondrial biogenesis, can give positive effect about the length and quality of life. The experiments done in this study demonstrated that male and female mice inoculated with the colon-rectal tumour and underwent to different training protocols (TR_P, TR_L, TR_M, TR_H), showed a similar trend in body weight loss. Cachectic male mice trained with moderate and high intensity training protocols survived longer than control groups. These data suggest that endurance exercise could be an adjuvant therapy for cancer survival, but it seems to be gender specific.

These observations on cachectic mice are only a first experimental approach; other experiments are necessary to confirm whether Hsp60 is lead up to its targets, promoting the PGC1α mediated response and encouraging formation of new fibres, regeneration of muscle tissue and body mass maintenance.

In conclusion, the new knowledges arising from this study, contribute to understand the role of Hsp60 in the muscular adaptations to exercise training. The findings about the release and traffic of Hsp60 towards specific sites could be important in the hypothesis to use Hsp60 like medical treatment, as exercise training mimetic, in muscle wasting conditions, such as cancer, heart failure and aging.

5 REFERENCES

Acharyya S, Butchbach ME, Sahenk Z, Wang H, Saji M, Carathers M, Ringel MD, Skipworth RJ, Fearon KC, Hollingsworth MA, Muscarella P, Burghes AH, Rafael-Fortney JA, Guttridge DC. Dystrophin glycoprotein complex dysfunction: a regulatory link between muscular dystrophy and cancer cachexia. Cancer Cell. 2005 Nov;8(5):421-32.

Anderson EJ, Neufer PD. Type II skeletal myofibres possess unique propertiesthat potentiate mitochondrial H(2)O(2) generation. Am J Physiol Cell Physiol. 2006 Mar;290(3):C844-51.

Arany Z. PGC-1 coactivators and skeletal muscle adaptations in health and disease. Curr Opin Genet Dev. 2008 Oct;18(5):426-34.

Arnold L, Henry A, Poron F, Baba-Amer Y, van Rooijen N, Plonquet A, Gherardi RK, Chazaud B. Inflammatory monocytes recruited after skeletal muscle injury switch into antiinflammatory macrophages to support myogenesis. J Exp Med. 2007 May 14;204(5):1057-69

Asakura A, Seale P, Girgis-Gabardo A, Rudnicki MA. Myogenic specification of side population cells in skeletal muscle. J Cell Biol. 2002 Oct 14;159(1):123-34.

Atherton PJ, Smith K. Muscle protein synthesis in response to nutrition and exercise. J Physiol. 2012 Mar 1;590(Pt 5):1049-57.

Aulino P, Berardi E, Cardillo VM, Rizzuto E, Perniconi B, Ramina C, Padula F, Spugnini EP, Baldi A, Faiola F, Adamo S, Coletti D. Molecular, cellular and physiological characterization of the cancer cachexia-inducing C26 colon carcinoma in mouse. BMC Cancer. 2010 Jul 8;10:363. doi: 10.1186/1471-2407-10-363.

Balon TW, Nadler JL. Nitric oxide release is present from incubated skeletal muscle preparations. J Appl Physiol (1985). 1994 Dec;77(6):2519-21.

Biressi S, Rando TA. Heterogeneity in the muscle satellite cell population. Semin Cell Dev Biol. 2010 Oct;21(8):845-54.

Bloemberg D, Quadrilatero J. Rapid determination of myosin heavy chain expression in rat, mouse, and human skeletal muscle using multicolor immunofluorescence analysis. PLoS One. 2012;7(4):e35273. doi: 10.1371/journal.pone.0035273. Epub 2012 Apr 18.

Bowen TS, Schuler G, Adams V. Skeletal muscle wasting in cachexia and sarcopenia: molecular pathophysiology and impact of exercise training. J Cachexia Sarcopenia Muscle. 2015 Sep;6(3):197-207.

Brack AS, Conboy IM, Conboy MJ, Shen J, Rando TA. A temporal switch from notch to Wnt signaling in muscle stem cells is necessary for normal adult myogenesis. Cell Stem Cell. 2008 Jan 10;2(1):50-9.

Brack AS, Conboy MJ, Roy S, Lee M, Kuo CJ, Keller C, Rando TA. Increased Wnt signaling during aging alters muscle stem cell fate and increases fibrosis. Science. 2007 Aug 10;317(5839):807-10.

Campanella C, Bucchieri F, Ardizzone NM, Marino Gammazza A, Montalbano A, Ribbene A, Di Felice V, Bellafiore M, David S, Rappa F, Marasà M, Peri G, Farina F, Czarnecka AM, Conway de Macario E, Macario AJ, Zummo G, Cappello F. Upon oxidative stress, the antiapoptotic Hsp60/procaspase-3 complex persists in mucoepidermoid carcinoma cells. Eur J Histochem. 2008 Oct-Dec;52(4):221-8.

Campanella C, Bucchieri F, Merendino AM, Fucarino A, Burgio G, Corona DF, Barbieri G, David S, Farina F, Zummo G, de Macario EC, Macario AJ, Cappello

F. The odyssey of Hsp60 from tumour cells to other destinations includes plasma membrane-associated stages and Golgi and exosomal protein-trafficking modalities. PLoS One. 2012;7(7):e42008.

Campanella C, Marino Gammazza A, Mularoni L, Cappello F, Zummo G, Di Felice V. A comparative analysis of the products of GROEL-1 gene from Chlamydia trachomatis serovar D and the HSP60 var1 transcript from Homo sapiens suggests a possible autoimmune response. Int J Immunogenet. 2009 Feb;36(1):73-8.

Cappello F, Conway de Macario E, Marasà L, Zummo G, Macario AJ. Hsp60 expression, new locations, functions and perspectives for cancer diagnosis and therapy. Cancer Biol Ther. 2008 Jun;7(6):801-9.

Cohen S, Nathan JA, Goldberg AL. Muscle wasting in disease: molecular mechanisms and promising therapies. Nat Rev Drug Discov. 2015 Jan;14(1):58-74.

Corbett TH, Griswold DP Jr, Roberts BJ, Peckham JC, Schabel FM Jr. Tumour induction relationships in development of transplantable cancers of the colon in mice for chemotherapy assays, with a note on carcinogen structure. Cancer Res. 1975 Sep;35(9):2434-9.

Costelli P, Bossola M, Muscaritoli M, Grieco G, Bonelli G, Bellantone R, Doglietto GB, Baccino FM, Rossi Fanelli F: Anticytokine treatment prevents the increase in the activity of ATP-ubiquitin- and Ca(2+)-dependent proteolytic systems in the muscle of tumour-bearing rats. Cytokine 2002; 19(1):1-5.

Courneya KS, Friedenreich CM. Physical activity and cancer control. Semin Oncol Nurs. 2007 Nov;23(4):242-52.

Dargelos E, Brulé C, Combaret L, Hadj-Sassi A, Dulong S, Poussard S, Cottin P. Involvement of the calcium-dependent proteolytic system in skeletal muscle aging. Exp Gerontol. 2007 Nov;42(11):1088-98.

Davies KJ, Quintanilha AT, Brooks GA, Packer L. Free radicals and tissue damage produced by exercise. Biochem Biophys Res Commun. 1982 Aug 31;107(4):1198-205.

De Angelis L, Berghella L, Coletta M, Lattanzi L, Zanchi M, Cusella-De Angelis MG, Ponzetto C, Cossu G. Skeletal myogenic progenitors originating from embryonic dorsal aorta coexpress endothelial and myogenic markers and contribute to postnatal muscle growth and regeneration. J Cell Biol. 1999 Nov 15;147(4):869-78.

Dellavalle A, Maroli G, Covarello D, Azzoni E, Innocenzi A, Perani L, Antonini S, Sambasivan R, Brunelli S, Tajbakhsh S, Cossu G. Pericytes resident in postnatal skeletal muscle differentiate into muscle fibres and generate satellite cells. Nat Commun. 2011 Oct 11;2:499.

Di Felice V, Ardizzone N, Marcianò V, Bartolotta T, Cappello F, Farina F, Zummo G. Senescence-associated HSP60 expression in normal human skin fibroblasts. Anat Rec A Discov Mol Cell Evol Biol. 2005 May;284(1):446-53.

Di Felice V, Macaluso F, Montalbano A, Gammazza AM, Palumbo D, Angelone T, Bellafiore M, Farina F. Effects of conjugated linoleic acid and endurance training on peripheral blood and bone marrow of trained mice. J Strength Cond Res. 2007 Feb;21(1):193-8.

Eley HL, Russell ST, Tisdale MJ: Effect of branched-chain amino acids on muscle atrophy in cancer cachexia. Biochem J 2007; 407(1):113-20.

Eley HL, Tisdale MJ: Skeletal muscle atrophy, a link between depression of protein synthesis and increase in degradation. J Biol Chem 2007; 282(10):7087-97.

Ellins, E. et al. The relationship between carotid stiffness and circulating levels of heat shock protein 60 in middle-aged men and women. Journal of hypertension 26, 2389-2392, doi:10.1097/HJH.0b013e328313918b (2008).

Evans WJ, Morley JE, Argilés J, Bales C, Baracos V, Guttridge D, Jatoi A, Kalantar-Zadeh K, Lochs H, Mantovani G, Marks D, Mitch WE, Muscaritoli M, Najand A, Ponikowski P, Rossi Fanelli F, Schambelan M, Schols A, Schuster M, Thomas D, Wolfe R, Anker SD. Cachexia: a new definition. Clin Nutr. 2008 Dec;27(6):793-9.

Febbraio MA, Mesa JL, Chung J, Steensberg A, Keller C, Nielsen HB, Krustrup P, Ott P, Secher NH, Pedersen BK. Glucose ingestion attenuates the exercise-induced increase in circulating heat shock protein 72 and heat shock protein 60 in humans. Cell Stress Chaperones. 2004 Winter;9(4):390-6

Fehrenbach E, Niess AM. Role of heat shock proteins in the exercise response. Exerc Immunol Rev. 1999;5:57-77.

Flanagan SW, Ryan AJ, Gisolfi CV, Moseley PL. Tissue-specific HSP70 response in animals undergoing heat stress. Am J Physiol. 1995 Jan;268(1 Pt 2):R28-32.

Folkesson M, Mackey AL, Langberg H, Oskarsson E, Piehl-Aulin K, Henriksson J, Kadi F. The expression of heat shock protein in human skeletal muscle: effects of muscle fibre phenotype and training background. Acta Physiol (Oxf). 2013 Sep;209(1):26-33. doi: 10.1111/apha.12124. Epub 2013 Jun 15.

Goodson ML, Park-Sarge OK, Sarge KD. Tissue-dependent expression of heat shock factor 2 isoforms with distinct transcriptional activities. Mol Cell Biol. 1995 Oct;15(10):5288-93.

Gussoni E, Soneoka Y, Strickland CD, Buzney EA, Khan MK, Flint AF, Kunkel LM, Mulligan RC. Dystrophin expression in the mdx mouse restored by stem cell transplantation. Nature. 1999 Sep 23;401(6751):390-4.

Hasselgren PO, Wray C, Mammen J: Molecular regulation of muscle cachexia: it may be more than the proteasome. Biochem Biophys Res Commun 2002; 290(1):1-10.

Irrcher I, Ljubicic V, Hood DA. Interactions between ROS and AMP kinase activity in the regulation of PGC-1alpha transcription in skeletal muscle cells. Am J Physiol Cell Physiol. 2009 Jan;296(1):C116-23.

Irrcher I, Ljubicic V, Kirwan AF, Hood DA. AMP-activated protein kinase-regulated activation of the PGC-1alpha promoter in skeletal muscle cells. PLoS One. 2008;3(10):e3614.

Jackson KA, Mi T, Goodell MA. Hematopoietic potential of stem cells isolated from murine skeletal muscle. Proc Natl Acad Sci U S A. 1999 Dec 7;96(25):14482-6.

Lenk K, Erbs S, Höllriegel R, Beck E, Linke A, Gielen S, Winkler SM, Sandri M, Hambrecht R, Schuler G, Adams V: Exercise training leads to a reduction of elevated myostatin levels in patients with chronic heart failure. Eur J Prev Cardiol 2012; 19(3):404-11.

Lenk K, Schuler G, Adams V: Skeletal muscle wasting in cachexia andsarcopenia: molecular pathophysiology and impact of exercise training. J Cachexia Sarcopenia Muscle 2010; 1(1):9-21.

Lewthwaite J, Owen N, Coates A, Henderson B, Steptoe A. Circulating human heat shock protein 60 in the plasma of British civil servants: relationship to physiological and psychosocial stress. Circulation. 2002 Jul 9;106(2):196-201.

Li YP, Chen Y, Li AS, Reid MB: Hydrogen peroxide stimulates ubiquitin-conjugating activity and expression of genes for specific E2 and E3 proteins in skeletal muscle myotubes. Am J Physiol Cell Physiol 2003; 285(4):C806 12.

Liu CM, Yang Z, Liu CW, Wang R, Tien P, Dale R, Sun LQ: Effect of RNA oligonucleotide targeting Foxo-1 on muscle growth in normal and cancer cachexia mice. Cancer Gene Ther 2007;14(12):945-52.

Liu Y, Steinacker JM. Changes in skeletal muscle heat shock proteins: pathological significance. Front Biosci. 2001 Jan 1;6:D12-25.

Locke M, Noble EG. Stress proteins: the exercise response. Can J Appl Physiol. 1995 Jun;20(2):155-67.

Locke M. The cellular stress response to exercise: role of stress proteins. Exerc Sport Sci Rev. 1997;25:105-36.

Lokireddy S, Wijesoma IW, Bonala S, Wei M, Sze SK, McFarlane C, Kambadur R, Sharma M: Myostatin is a novel tumoural factor that induces cancer cachexia. Biochem J 2012; 446(1):23-36.

Lorite MJ, Smith HJ, Arnold JA, Morris A, Thompson MG, Tisdale MJ: Activation of ATP-ubiquitin-dependent proteolysis in skeletal muscle in vivo and murine myoblasts in vitro by a proteolysis-inducing factor (PIF). Br J Cancer 2001; 85(2):297-302.

Macaluso F, Brooks NE, Niesler CU, Myburgh KH. Satellite cell pool expansion is affected by skeletal muscle characteristics. Muscle Nerve. 2013 Jul;48(1):109-16.

Manzerra P, Rush SJ, Brown IR. Tissue-specific differences in heat shockprotein hsc70 and hsp70 in the control and hyperthermic rabbit. J Cell Physiol. 1997 Feb;170(2):130-7.

Marino Gammazza A, Rizzo M, Citarrella R, Rappa F, Campanella C, Bucchieri F, Patti A, Nikolic D, Cabibi D, Amico G, Conaldi PG, San Biagio PL, Montalto G, Farina F, Zummo G, Conway de Macario E, Macario AJ, Cappello F. Elevated blood Hsp60, its structural similarities and cross-reactivity with thyroid molecules, and its presence on the plasma membrane of oncocytes point to the chaperonin as an immunopathogenic factor in Hashimoto's thyroiditis. Cell Stress Chaperones. 2014 May;19(3):343-53.

Martini F, Timmons M, Tallitsch R. Anatomia Umana. EdiSES 2012.

Mattson JP, Ross CR, Kilgore JL, Musch TI. Induction of mitochondrial stress proteins following treadmill running. Med Sci Sports Exerc. 2000 Feb;32(2):365-9.

McArdle A, Dillmann WH, Mestril R, Faulkner JA, Jackson MJ. Overexpression of HSP70 in mouse skeletal muscle protects against muscle damage and age-related muscle dysfunction. FASEB J. 2004 Feb;18(2):355-7.

McArdle A, van der Meulen J, Close GL, Pattwell D, Van Remmen H, Huang TT, Richardson AG, Epstein CJ, Faulkner JA, Jackson MJ. Role of mitochondrial superoxide dismutase in contraction-induced generation of reactive oxygen species in skeletal muscle extracellular space. Am J Physiol Cell Physiol. 2004 May;286(5):C1152-8.

McCroskery S, Thomas M, Maxwell L, Sharma M, Kambadur R. Myostatin negatively regulates satellite cell activation and self-renewal. J Cell Biol. 2003 Sep 15;162(6):1135-47.

McMullen CA, Ferry AL, Gamboa JL, Andrade FH, Dupont-Versteegden EE. Age-related changes of cell death pathways in rat extraocular muscle. Exp Gerontol. 2009 Jun-Jul;44(6-7):420-5.

Miura S, Kai Y, Kamei Y, Ezaki O. Isoform-specific increases in murine skeletal muscle peroxisome proliferator-activated receptor-gamma coactivator-1alpha (PGC-1alpha) mRNA in response to beta2-adrenergic receptor activation and exercise. Endocrinology. 2008 Sep;149(9):4527-33.

Montarras D, Morgan J, Collins C, Relaix F, Zaffran S, Cumano A, Partridge T, Buckingham M. Direct isolation of satellite cells for skeletal muscle regeneration. Science. 2005 Sep 23;309(5743):2064-7.

Morimoto RI, Sarge KD, Abravaya K. Transcriptional regulation of heat shock genes. A paradigm for inducible genomic responses. J Biol Chem. 1992 Nov 5;267(31):21987-90.

Morton JP, Maclaren DP, Cable NT, Campbell IT, Evans L, Kayani AC, McArdle A, Drust B. Trained men display increased basal heat shock protein content of skeletal muscle. Med Sci Sports Exerc. 2008 Jul;40(7):1255-62

Moseley PL. Heat shock proteins and heat adaptation of the whole organism. J Appl Physiol (1985). 1997 Nov;83(5):1413-7.

Muliawati Y, Haroen H, Rotty LW: Cancer anorexia - cachexia syndrome. Acta Med Indones 2012 ;44(2):154-62.

Murphy MM, Lawson JA, Mathew SJ, Hutcheson DA, Kardon G. Satellite cells, connective tissue fibroblasts and their interactions are crucial for muscle regeneration. Development. 2011 Sep;138(17):3625-37.

Neufer PD, Ordway GA, Hand GA, Shelton JM, Richardson JA, Benjamin IJ, Williams RS. Continuous contractile activity induces fibre type specific expression of HSP70 in skeletal muscle. Am J Physiol. 1996 Dec;271(6 Pt1):C1828-37.

Oishi Y, Taniguchi K, Matsumoto H, Ishihara A, Ohira Y, Roy RR. Differential responses of HSPs to heat stress in slow and fast regions of rat *gastrocnemius* muscle. Muscle Nerve. 2003 Nov;28(5):587-94.

Ornatsky OI, Connor MK, Hood DA. Expression of stress proteins and mitochondrial chaperonins in chronically stimulated skeletal muscle. Biochem J. 1995 Oct 1;311 (Pt 1):119-23. PubMed PMID: 7575442.

Osterziel KJ, Strohm O, Schuler J, Friedrich M, Hänlein D, Willenbrock R, Anker SD, Poole-Wilson PA, Ranke MB, Dietz R: Randomised, double-blind, placebo-controlled trial of human recombinant growth hormone in patients with chronic heart failure due to dilated cardiomyopathy. Lancet 1998; 351(9111):1233-7.

Pallafacchina G, Blaauw B, Schiaffino S. Role of satellite cells in muscle growth and maintenance of muscle mass. Nutr Metab Cardiovasc Dis. 2013 Dec;23 Suppl 1:S12-8.

Pannérec A, Marazzi G, Sassoon D. Stem cells in the hood: the skeletal muscle niche. Trends Mol Med. 2012 Oct;18(10):599-606.

Pockley AG, Bulmer J, Hanks BM, Wright BH. Identification of human heat shock protein 60 (Hsp60) and anti-Hsp60 antibodies in the peripheral circulation of normal individuals. Cell Stress Chaperones. 1999 Mar;4(1):29-35

Powers SK, Talbert EE, Adhihetty PJ. Reactive oxygen and nitrogen species as intracellular signals in skeletal muscle. J Physiol. 2011 May 1;589(Pt9):2129-38.

Rea IM, McNerlan S, Pockley AG. Serum heat shock protein and anti-heat shock protein antibody levels in aging. Exp Gerontol. 2001 Feb;36(2):341-52.

Roberts BM, Ahn B, Smuder AJ, Al-Rajhi M, Gill LC, Beharry AW, Powers SK, Fuller DD, Ferreira LF, Judge AR. Diaphragm and ventilatory dysfunction during cancer cachexia. FASEB J. 2013 Jul;27(7):2600-10.

Ruas JL, White JP, Rao RR, Kleiner S, Brannan KT, Harrison BC, Greene NP, Wu J, Estall JL, Irving BA, Lanza IR, Rasbach KA, Okutsu M, Nair KS, Yan Z, Leinwand LA, Spiegelman BM. A PGC-1α isoform induced by resistance training regulates skeletal muscle hypertrophy. Cell. 2012 Dec 7;151(6):1319-31.

Sakellariou GK, Davis CS, Shi Y, Ivannikov MV, Zhang Y, Vasilaki A, Macleod GT, Richardson A, Van Remmen H, Jackson MJ, McArdle A, Brooks SV. Neuron-specific expression of CuZnSOD prevents the loss of muscle mass and function that occurs in homozygous CuZnSOD-knockout mice. FASEB J. 2014 Apr;28(4):1666-81.

Samelman TR. Heat shock protein expression is increased in cardiac and skeletal muscles of Fischer 344 rats after endurance training. Exp Physiol. 2000 Jan;85(1):92-102.

Sato N, Michaelides MC, Wallack MK. Characterization of tumourigenicity, mortality, metastasis, and splenomegaly of two cultured murine colon lines. Cancer Res. 1981 Jun;41(6):2267-72.

Smart NA, Steele M: The effect of physical training on systemic proinflammatory cytokine expression in heart failure patients: a systematic review. Congest Heart Fail 2011; 17(3):110-4.

Sonnet C, Lafuste P, Arnold L, Brigitte M, Poron F, Authier FJ, Chrétien F, Gherardi RK, Chazaud B. Human macrophages rescue myoblasts and myotubes from apoptosis through a set of adhesion molecular systems. J Cell Sci. 2006 Jun 15;119(Pt 12):2497-507.

Sorger PK. Heat shock factor and the heat shock response. Cell. 1991 May 3;65(3):363-6.

Standring S. Anatomia del Gray. ELSEVIER 2009.

Tanhauser SM, Laipis PJ. Multiple deletions are detectable in mitochondrial DNA of aging mice. J Biol Chem. 1995 Oct 20;270(42):24769-75.

Tisdale MJ: Clinical anticachexia treatments. Nutr Clin Pract 2006;21(2):168-74.

Tisdale MJ: Mechanisms of cancer cachexia. Physiol Rev 2009; 89(2):381-410.

Welch WJ. Mammalian stress response: cell physiology, structure/function of stress proteins, and implications for medicine and disease. Physiol Rev. 1992 Oct;72(4):1063-81.

Wen X, Wu J, Chang JS, Zhang P, Wang J, Zhang Y, Gettys TW, Zhang Y. Effect of exercise intensity on isoform-specific expressions of NT-PGC-1 α mRNA in mouse skeletal muscle. Biomed Res Int. 2014;2014:402175.

Wenz T, Rossi SG, Rotundo RL, Spiegelman BM, Moraes CT. Increased muscle PGC-1alpha expression protects from sarcopenia and metabolic disease during aging. Proc Natl Acad Sci U S A. 2009 Dec 1;106(48):20405-10.

White JP, Gao S, Puppa MJ, Sato S, Welle SL, Carson JA. Testosterone regulation of Akt/mTORC1/FoxO3a signaling in skeletal muscle. Mol Cell Endocrinol. 2013 Jan 30;365(2):174-86.

Wing SS. Deubiquitinases in skeletal muscle atrophy. Int J Biochem Cell Biol. 2013 Oct;45(10):2130-5.

Xu Q, Schett G, Perschinka H, Mayr M, Egger G, Oberhollenzer F, Willeit J, Kiechl S, Wick G. Serum soluble heat shock protein 60 is elevated in subjects with atherosclerosis in a general population. Circulation. 2000 Jul 4;102(1):14-20.

Yuan J, Dunn P, Martinus RD. Detection of Hsp60 in saliva and serum from type 2 diabetic and non-diabetic control subjects. Cell Stress Chaperones. 2011 Nov;16(6):689-93. doi: 10.1007/s12192-011-0281-7. Epub 2011 Jul 13.

Zhang X, He M, Cheng L, Chen Y, Zhou L, Zeng H, Pockley AG, Hu FB, Wu T. Elevated heat shock protein 60 levels are associated with higher risk of coronary heart disease in Chinese. Circulation. 2008 Dec 16;118(25):2687-93.

Zhou X, Wang JL, Lu J, Song Y, Kwak KS, Jiao Q, Rosenfeld R, Chen Q, Boone T, Simonet WS, Lacey DL, Goldberg AL, Han HQ: Reversal of cancer cachexia and muscle wasting by ActRIIB antagonism leads to prolonged survival. Cell 2010; 142(4):531-43.